Proceedings

Fifteenth ACC Cyfronet AGH HPC Users' Conference

KU KDM 2023

Editors: Kazimierz Wiatr
Jacek Kitowski
Marian Bubak

Zakopane, 19-21 April 2023

Proceedings

Fifteenth
ACC Cyfronet AGH
HPC Users'
Conference

Zakopane
19-21 April 2023

Editors: Kazimierz Wiatr
Jacek Kitowski
Marian Bubak

Published in April 2023

by Academic Computer Centre Cyfronet AGH
Nawojki 11, 30-950 Kraków, P.O. Box 386, Poland

ISBN 978-83-61433-37-8

Cover design and book typesetting by Joanna Kasina.

Ladies and Gentlemen!

This year's High Performance Computers Users' Conference – KU KDM 2023 – is the fifteenth such meeting. It also coincides with a special event – the celebration of the 50th anniversary of Cyfronet. Additionally, after two editions organised online, we are returning to a direct meeting in Zakopane.

The last 50 years have brought intense technological, social, and economic changes. Hence Cyfronet, while continuing its mission to provide IT support for the scientific community, constantly develops its competencies. We maintain a permanent dialogue with representatives of science and with companies offering high-end solutions regarding software and IT hardware. The result is an attempt to respond to the ever-growing demand of science and innovative economy for computing power, memory resources and specialised software. The expanded and modernised IT infrastructure of Cyfronet, including, above all, supercomputers, is to serve this purpose.

Our newest supercomputer, Athena, is currently the fastest supercomputer in Poland. Athena provides the Polish scientific community and innovative economy with computing resources based on the latest processors, GPGPU accelerators, and the essential data storage sub-system based on high-speed flash memory. Athena's configuration covers servers with AMD EPYC CPUs and NVIDIA A100 GPGPU cards. The internal communication is provided by the Infiniband HDR (200 Gb/s) network. Athena's theoretical computing power is over 7.7 PF, three times more than Prometheus. That allowed the computer to appear in 105th and then 113th place in the TOP500 list of the world's fastest supercomputers, respectively in June and November 2022. Athena creates extraordinary capabilities if computing for AI is considered, as it offers 240 PF for such applications. An excellent computing power-to-electricity consumption ratio also characterises the supercomputer. That was underlined when in 2022 Athena took respectively 9th and 17th place in the Green500 list of the most energy-efficient supercomputers in the world.

Recent Green500 lists also included another Cyfronet supercomputer – Ares, which has occupied 83rd and then 94th place. Ares is built out of a set of computing servers with a computing power of over 3.5 PF and the disc sub-system of a capacity of over 11 PB. The supercomputer has 37 824 computing cores (Intel Xeon Platinum processors) and 147.7 TB RAM. It is equipped with computationally efficient GPGPU NVIDIA Tesla V100 cards. Thanks to the innovative cooling system, the heat removed from Ares is used to heat the rooms in the Data Centre Podole. In the TOP500 list, Ares subsequently occupied 290th and 323rd place.

Prometheus, which in the period from 2015 till the mid-2020 was the fastest supercomputer in Poland, keeps offering over 50 000 computational cores (energy-saving and efficient Intel Haswell and Intel Skylake processors) with the computing power of 2.4 PF, the GPGPU processors in computational nodes connected by the fast Infiniband QDR network and fast disc resources equipped with the efficient LUSTRE file system, all that to serve the needs of calculations for scientific projects. Additionally, Prometheus has a computing system dedicated to the needs of artificial intelligence, with a computational power of over 4 PF. That system is composed of the HPE Apollo 6500 servers, equipped with the Intel Xeon Gold 5220 processors and NVIDIA Tesla V100 accelerators. In June 2022, Prometheus was announced as 476th in the TOP500 list and 162nd in the Green500 list.

The intensity of Users' use of supercomputers is evidenced by the sum of computing tasks performed in just one year on these three machines, which exceeds 6 million. However, the constantly growing demand of Polish science for computing resources drives us to develop these resources continuously. In this context, the planned installation of a new supercomputer with computing power at least several times higher than that of Athena scheduled for this year, is worth mentioning. Like all those operating in Cyfronet, the new computer will be available via the PLGrid Portal.

Cyfronet is also a part of numerous essential initiatives, both on Polish and European grounds, creating new opportunities for science and society. As a coordinator of the PLGrid

Consortium, it plays the leading role in two initiatives included in the Polish Roadmap for Research Infrastructures (PMIB). Within the *National Supercomputing Infrastructure for EuroHPC – EuroHPC PL* Cyfronet is the coordinator of this project and the leader of the Consortium and builds, together with six Partners, a specialised general-purpose infrastructure for large-scale computing. *EuroHPC PL* will allow Polish researchers to use cutting-edge supercomputer technologies and the resources of quantum computers and neuromorphic accelerators. In turn, within the *National PLGrid Cloud Infrastructure for EOSC,* Cyfronet co-creates the project of the globally accessible and multidisciplinary environment, in which scientists, innovators, the innovative economy as well as the whole society will be able to conveniently publish and benefit from the data, tools and results of scientific papers for research, innovation and education.

An important task in recent years has been the coordination of Polish activity in the LUMI consortium that includes 10 European states. That effort aims to make the LUMI supercomputer, which since 2022 has been the fastest computer in Europe and third in the world by the TOP500 list, accessible for Polish scientists. After the successful completion of the pilot phase, LUMI became fully operational. Since then, domestic researchers can be awarded regular access to its resources via the PLGrid Portal under competitions organised by Cyfronet.

The employees of our Centre aim to search for and implement the best possible solutions to serve you – the Users of computational and storage resources and software. That requires constant information exchange. That is why the Conference of the Users serves as an excellent opportunity to present and recognise the research results in the areas that have and will continue to significantly impact the environment, economy and society. It is also an opportunity for a direct debate with the Users and for becoming up to date with the research challenges they face to resolve them together.

The Conference will focus on large-scale calculations and simulations, parallel analysis of big data, utilisation of AI methods, new algorithms in IT as well as tools and techniques in HPC systems. The most important part is the presentation of research results carried out with the support of our Centre's computing resources and software being shared. Additionally, we will present information concerning Cyfronet's current activities and plans, new possibilities brought by the PLGrid infrastructure, including cloud and AI, the new directions for developing computer and network architectures as well as information from suppliers of equipment and software installed in Cyfronet.

For almost 50 years, Cyfronet has been an integral part of the ecosystem of Polish and international science. Thus our work comes with great responsibility. With it in mind, we carefully listen to the Users' needs. We hope that KU KDM 2023 will provide us with numerous opportunities for flourishing discussions between researchers working in various scientific fields and implementing varied and interesting scientific methods. We are convinced that such an exchange of experiences will allow for a broad, interdisciplinary and multidisciplinary perspective on current research directions.

I would like to thank all the Users for cooperation in improving our services and creating new directions for our development! I cordially invite you to participate in the fifteenth HPC Users' Conference. I would like to wish fruitful discussions and new research ideas to all the Participants.

With best regards,
Kazimierz Wiatr

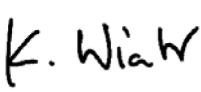

Cyfronet Director

Organization

KU KDM 2023 was organized by the Academic Computer Centre Cyfronet AGH University of Science and Technology, Nawojki 11, 30-950 Kraków, Poland.

Organizing Committee

Kazimierz Wiatr, Mariola Czuchry, Tomasz Gunia, Joanna Kasina, Kamil Mucha, Robert Pająk

KU KDM'23 Program Committee

Kazimierz Wiatr (chairman)	Academic Computer Centre Cyfronet AGH
Krzysztof Boryczko	Institute of Computer Science AGH
Marian Bubak	Institute of Computer Science AGH / Academic Computer Centre Cyfronet AGH
Joanna Dulińska	Cracow University of Technology
Łukasz Dutka	Academic Computer Centre Cyfronet AGH
Armen Edigarian	Jagiellonian University
Andrzej Eilmes	Jagiellonian University
Marek Gorgoń	Department of Automatics and Robotics AGH
Stanisław Jadach	Institute of Nuclear Physics PAN
Ernest Jamro	Institute of Electronics AGH / Academic Computer Centre Cyfronet AGH
Marek Jarnicki	Jagiellonian University
Zbigniew Kąkol	Department of Solid State Physics AGH
Marek Kisiel-Dorohinicki	Institute of Computer Science AGH
Jacek Kitowski	Institute of Computer Science AGH / Academic Computer Centre Cyfronet AGH
Antoni Ligęza	Department of Applied Computer Science AGH
Grzegorz Mazur	Jagiellonian University
Janusz Mrozek	Jagiellonian University
Janusz Orkisz	Cracow University of Technology
Łukasz Rauch	Department of Applied Computer Science and Modelling AGH
Irena Roterman-Konieczna	Jagiellonian University Medical College
Paweł Russek	Institute of Electronics AGH / Academic Computer Centre Cyfronet AGH
Marek Skomorowski	Jagiellonian University
Renata Słota	Institute of Computer Science AGH
Marek Stanuszek	Cracow University of Technology
Mariusz Sterzel	Academic Computer Centre Cyfronet AGH
Tomasz Szmuc	Department of Applied Computer Science AGH
Piotr Tworzewski	Jagiellonian University

Sponsoring Institutions

Hewlett Packard Enterprise
Advanced Micro Devices
Atos
DataDirect Networks

Table of Contents

Contributed Papers

Ab Initio Molecular Dynamics Studies of Hydrogen Bonding and IR Spectra in EMIM-TFSI/H_2O Systems

Piotr Wróbel, Piotr Kubisiak, Andrzej Eilmes

Jagiellonian University, Faculty of Chemistry, Gronostajowa 2, 30-387 Kraków, Poland

piotr.wrobel@doctoral.uj.edu.pl, {kubisiak, eilmes}@chemia.uj.edu.pl

Keywords: ionic liquids, molecular dynamics, hydrogen bonding, infrared spectroscopy

1. Introduction

Ionic liquids are organic salts, molten at ambient temperature. They are the subject of research on alternative solvents, e.g. for electrolytes for batteries. Due to their character, strong electrostatic interactions dominate between the ions. However, in experimental conditions, a situation when an ionic liquid is contaminated by water is quite common. Then, also weak interactions, such as hydrogen bonds, are important for the properties of the solvent [1].

2. Description of the problem

Our aim was to analyse the statistics of hydrogen bonding in systems with different amounts of water in EMIM-TFSI ionic liquid. In addition, we wanted to obtain theoretical infrared spectra of such systems and analyse selected vibrations to check how the vibrational frequencies correlate with the formation of the hydrogen bonds.

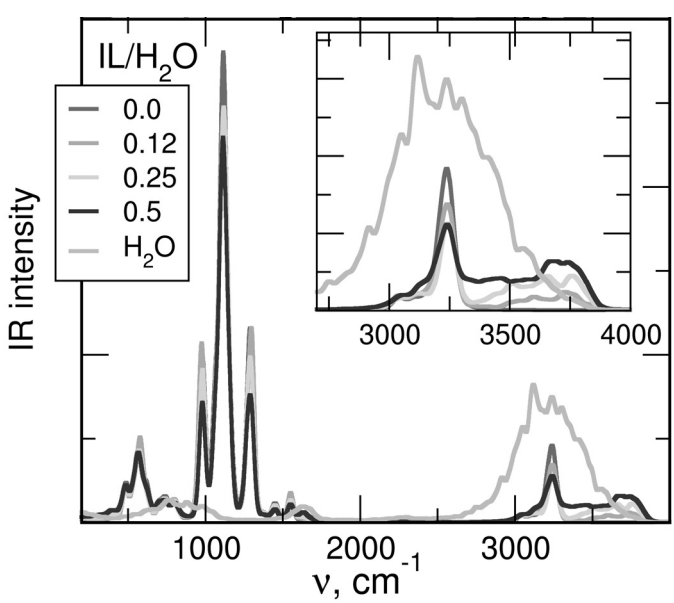

Fig. 1. Simulated IR spectra for EMIM-TFSI/H_2O systems with different molar fraction of water and for the bulk water.

3. Solution of the problem

In order to obtain information about hydrogen bonding and calculate theoretical infrared spectra, ab initio MD (AIMD) simulations were performed in the CP2K package [2] with PBE functional, Goedecker's pseudopotentials, molecularly optimised DZVP basis set, in the NVT ensemble using the Nosé-Hoover thermostat at T = 298 K.

4. Conclusions

Obtained theoretical IR spectra stood in a good agreement with experimental results. Examples of such spectrum are presented in Fig. 1. Comparison of oscillations for individual O-H and C-H bonds have shown correlations between the hydrogen bond formation and the vibrational frequencies. It has also indicated that changes observed in the region of O-H stretching frequency result from changing the number of water-water hydrogen bonds in the system.

Acknowledgements. The numerical experiment was possible through computing allocation on the Prometheus system at ACC Cyfronet AGH under the grants plgaenael6. All simulations were running on 96 cores and took about 4.4 M normalised walltime hours.

References

1. K. Fumino, et al.: The influence of hydrogen bonding on the physical properties of ionic liquids, in Phys. Chem. Chem. Phys. 2011, 13, 14064-14075.
2. J. Hutter, M. Iannuzzi, F. Schiffmann, J. VandeVodele: CP2K: Atomistic Simulations of Condensed Matter Systems, in WIREs Comput. Mol. Sci. 2014, 4, 15–25.
3. P. Wróbel, P. Kubisiak, A. Eilmes: Hydrogen Bonding and Infrared Spectra of Ethyl-3-methylimidazolium Bis(trifluoromethylsulfonyl)imide/Water Mixtures: A View from Molecular Dynamics Simulations, in J. Phys. Chem. B 2022, 126, 51, 10922-10932.

Vibrational Spectra from Molecular Dynamics: Seeking for an Efficient Computational Method

Andrzej Eilmes, Piotr Wróbel, Piotr Kubisiak

Jagiellonian University, Faculty of Chemistry, Gronostajowa 2, 30-387 Kraków, Poland

{eilmes, kubisiak}@chemia.uj.edu.pl, piotr.wrobel@doctoral.uj.edu.pl

Keywords: vibrational spectra, molecular dynamics, DFTB, GPU computing

1. Introduction

Vibrational spectroscopy (IR or Raman) is commonly used to study the effects of interactions in solution. Molecular dynamics (MD) simulations may be used to calculate the vibrational spectra in the condensed phase, including the effects of the solvent. Such a methodology has been recently applied by us to several systems: ionic liquids and electrolytes for metal-ion batteries [1-4].

2. Description of the problem

The IR or Raman spectrum can be obtained as a Fourier transform of the dipole moment or polarizability of the system, respectively, recorded in the MD run. Unfortunately, force field based MD usually is not accurate enough to provide satisfactory reproduction of the spectrum, therefore computationally expensive ab initio MD (AIMD) has to be used. When the Raman spectra are requested, additional computational cost needed for polarizability calculations is incurred. Therefore, the computational effort limits the usability of AIMD in modeling the vibrational spectra.

3. Solution of the problem

We used two approaches to reduce the computational cost of MD simulations. We tested several available parameterizations of the semiempirical Density Functional-based Tight Binding (DFTB) methodology, less demanding than the Density Functional Theory (DFT) calculations. The DFTB+ v. 22.1 software [5] was used with general purpose parameter sets *3ob*, *matsci*, *ob2*, broadly parameterized GFN-xTB variants, and also with specific parameterizations developed for bulk water.

The other solution was to use the GPU acceleration of AIMD simulations employing DFT methodology. Such calculations with the PBE functional and the 631+G* basis set were performed for explicitly solvated ion aggregates using Terachem v. 1.93 software [6] running on Nvidia Tesla K40d GPUs. In this variant of MD simulations also the polarizability tensors (and corresponding Raman spectra) were calculated for selected systems.

4. Conclusions

The quality of spectra obtained from the DFTB calculations depends heavily on the parameterization. The tailored parameterizations outperform general purpose sets, but are not readily available. From the general parameterizations, the most promising was the GFN2-xTB variant.

The advantages of the GPU-accelerated DFT simulations are the easy applicability to all systems for which the selected basis set is available and the possibility of computation of Raman spectrum in a reasonable time. Nevertheless, the size of the studied system is rather limited.

Acknowledgements. The numerical experiment was possible through computing allocation on the Prometheus system at ACC Cyfronet AGH under the grants plgaenael4, plgaenael6, plgaegpu2 and plgaegpu3. The CPU-based DFTB computations were running on 96 CPU cores and consumed about 1.2 M normalized walltime hours. The GPU-based simulations used 0.1 M walltime hours.

References

1. P. Wróbel, P. Kubisiak, A. Eilmes: MeTFSI (Me = Li, Na) Solvation in Ethylene Carbonate and Fluorinated Ethylene Carbonate: A Molecular Dynamics Study, in J. Phys. Chem. B, 2021, 125, 1248-1258.
2. P. Wróbel, P. Kubisiak, A. Eilmes: Hydrogen Bonding and Infrared Spectra of Ethyl-3-methylimidazolium Bis(trifluoromethylsulfonyl)imide/Water Mixtures: A View from Molecular Dynamics Simulations, in J. Phys. Chem. B 2022, 126, 10922-10932.
3. A. Eilmes, W. A. Alves: Theory-experiment partnership applied to the spectroscopic analysis of a promising conditioning-free electrolyte for Mg batteries, in J. Mol. Liquids 2022, 350, 118528.
4. A. Eilmes, W. A. Alves: Unraveling the solvates in a diethylene glycol dimethyl ether-based electrolyte: A computational-experimental contribution to Mg battery area, in J. Mol. Liquids 2022, 359, 119251.
5. B. Hourahine et al.: DFTB+, a Software Package for Efficient Approximate Density Functional Theory Based Atomistic Simulations, in J. Chem. Phys. 2020, 152, 124101.
6. Terachem v. 1.93, `http://www.petachem.com/`

Computational Modeling of Intermolecular Interactions in Supramolecular Crystals: Towards Automated Explorations of Chemical Spaces

Grzegorz Niedzielski, Robert Podgajny, James Hooper

Faculty of Chemistry, Jagiellonian University, Gronostajowa 2, 30-387 Kraków, Poland

grzegorz.niedzielski@doctoral.uj.edu.pl,
{robert.podgajny, james.hooper}@uj.edu.pl

Keywords: molecular crystals, anion-π interaction, density functional theory

1. Introduction

Supramolecular crystals designed from constituents with known properties are a hot research area, for example, to find a class of related materials that collectively exhibit a range of photophysical properties or to seek systems that inherently exhibit multiple interesting chemical phenomena. Their design allows for the manipulation of a material's properties by slightly modifying the composition and extent of interactions between constituents (potentially via polymorphism). It is well known that there has been success in the design of new materials by carefully choosing the precursors [1].

2. Description of the problem

One group of such materials that we have recently explored are those focused on the inclusion of anion-π interactions in supramolecular architectures [2, 3]. Our studies on these systems provide an opportunity to help with future efforts of exploring effective algorithms capable of predicting the important aspects of potential crystalline systems from simulations alone. To do so, we first analyzed how well results from molecular cluster models relate to the observed physicochemical properties, and, second, we implemented simple computational schemes that can detect how perturbations around a molecule within a cluster or a supramolecular environment influence its key electronic properties. The simulations were run on recently characterized supramolecular crystal structures with built-in anion-π intermolecular contacts. The subsequent calculations were also used to determine the extent of the influence of anion-π interactions on the observed properties.

3. Solution of the problem

Computations of electronic structure properties were done using popular density functional theory chemistry methods (with the PBE and B3LYP functionals), and most assessments of intermolecular binding within the crystal were done with the semiempirical PM7 and GFN1-xTB methods, all as they are implemented in the Amsterdam Modeling Suite (AMS) version 2021.

The semiempirical methods were used to analyze the strengths of every intermolecular interaction in the crystal structures, and then further used, with implicit solvation models, to comment on the likely geometries of prominent motifs from solution. To this aim, Python scripts were developed and assembled to extract and analyze all nearest neighbor pairs of molecules, primarily by studying the interaction energies between them.

The electronic structures were all primarily assessed by considering molecular contributions to the densities of states and using the results as the bases to extract molecular cluster for further analysis of spectroscopic properties with TD-DFT methods. Furthermore, DFT-gene-

rated electronic structures of the molecular clusters and of the supramolecular crystals were analyzed with ETS-NOCV analysis, NCIplot analysis, and considerations of various topological functions along key contacts in the structures (Fig. 1.).

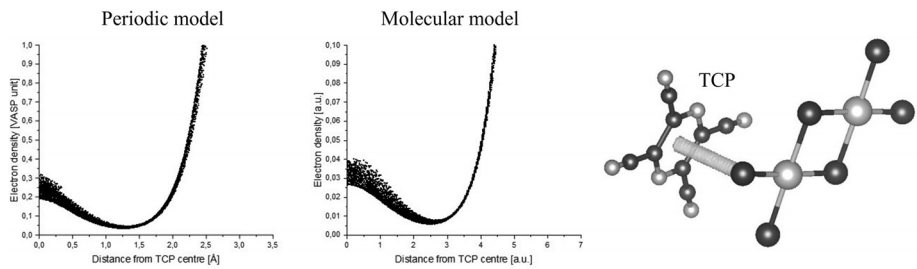

Fig. 1. Comparison between the electron density obtained using the periodic model (left side) and a molecular model (middle), along the shown contact (right).

4. Conclusions

It was found that the density functional methods were well able to reproduce and rationalize the key differences observed in the absorption spectra of the considered systems, and that charge transfer processes along the anion-pi contact were crucial among them. The probes of topological functions along key contacts within the crystal revealed that the molecular models were all well reproducing the electronic structure features along the non-covalent contacts in the crystal structures.

The semi-empirical methods were found to agree in general terms about the relative strengths of the (pair-wise) intermolecular interactions. Also, they indicated the importance and the anion-π contacts in stabilizing the crystal structures. Discrepancies were noticed, however, when the inclusion of implicit solvation models was considered, namely that parameterizations for similar solvents within the methods would lead to different qualitative fingerprints of the interactions.

Taken together, the implemented analytical tools are currently being adapted into computational mechanisms that aim to design new materials by modifying or substituting constituents within the greater framework.

Acknowledgements. This work/research has been supported by the National Science Centre (Poland) research project no. UMO-2019/35/B/ST5/01481. The numerical experiment was possible through computing allocation on the Prometheus and Ares systems at ACC Cyfronet AGH under the grants plgsoliddft2022 and plgsoliddft2023.

References

1. Zakrzewski, J.; Liberka. M.; Żychowicz, M.; Chorąży, S.; Diverse physical functionalities of rare-earth hexacyanidometallate frameworks and their molecular analogues, *Inorg. Chem. Front.*, 2021, 8, 452-483.
2. Kuźniak-Glanowska, E.; Głosz, D.; Niedzielski, G.; Kobylarczyk, J.; Srebro-Hooper, M.; Hooper, J.; Podgajny R.; Binding of Anionic Pt(II) Complexes in a Dedicated Organic Matrix: towards New Binary Crystalline Composites, *Dalt. Trans.* 2021, 50, 170–185.
3. Kobylarczyk, J.; Pinkowicz, D.; Srebro-Hooper, M.; Hooper, J.; Podgajny, R.; Anion-π architectures of HAT$(CN)_6$ and 5d polycyanidometalates: $[W(CN)_8]^{3-}$, $[Re(CN)_7]^{3-}$, and $[Pt(CN)_6]^{2-}$, *Crys. Growth. Des.,* 2019, 19, 1215-1225.

Molecular Modeling of Cisplatin Derivatives: the Relationship Between Structure and Potential Bioactivity

Wojciech M. Łach, Marta M. Solarek, Maria Nowakowska,
Krzysztof Szczubiałka, Mateusz Z. Brela

Jagiellonian University, Faculty of Chemistry, Gronostajowa 2, 30-387 Kraków, Poland

wojciech.lach@student.uj.edu.pl, marta.stolarek@doctoral.uj.edu.pl,
[maria.nowakowska, krzysztof.szczubialka, mateusz.brela]@uj.edu.pl

Keywords: cisplatin, photopharmacology, structure-activity relationship, energy decomposition analysis, molecular electrostatic potential

1. Introduction

One of the most famous anticancer drugs, and the first including transition metal, is cisplatin. This small complex has accidentally been discovered to have a cytotoxic effect on cells and is used as an anticancer agent to this day. Its activity on tumor cells is mostly associated with the creation of DNA-Pt adducts, which leads to double helix deformation and activation of biochemical programmed cell death pathways. This complex mechanism begins with the activation of the drug molecule by the replacement of two chloride anions with more dissociative water molecules. Activated cisplatin is a strong electrophile and reacts with biological nucleophiles, not only nucleic acids. Its reactivity is the reason for the occurrence of side effects, from which the most specific ones are nephrotoxicity and ototoxicity. Improving life comfort during cisplatin therapy is now the main issue driving the designing new complex derivatives [1].

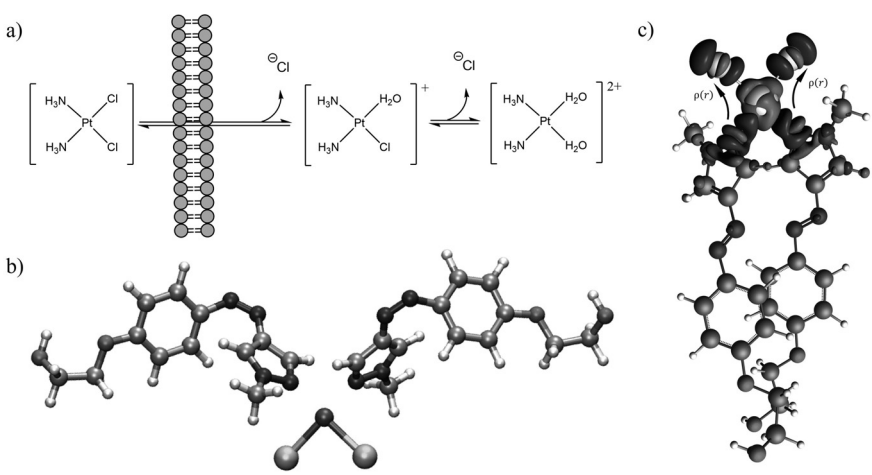

Fig. 1. a) Scheme presenting cisplatin activation mechanism. b) Model of proposed cisplatin derivative containing molecular groups able to change conformation due to specific wavelength irradiation c) The deformation density Δρ(r) (isovalue: 0.003) visualizing the charge transfer between two considered fragments: the $PtCl_2$ and two photoswitchable ligands.

The mentioned side effects could be limited by shortening the exposition of the cytotoxic drug on healthy cells. One way of controlling compounds' cytotoxicity is proposed in the as-

sumptions of photopharmacology. One of the main goals of this scientific field is the creation of a compound that can change the structural properties (e.g., E-Z conformation) due to light irradiation. As a result of that change, the bioactivity of the molecule will also differ [2]. Designation of a structure, which can be activated with visible light and only in a specific time and place in an organism, will give the promise for burdened with side effects therapies, like e.g., cisplatin therapy.

2. Description of the problem

The main goal of the presented research is to combine the assumptions of photopharmacology and structural requirements for the preservation of the cisplatin-like mechanism of action. The proposed molecule should have a similar structure to cisplatin, as well as the ability to change bioactivity due to light irradiation. Molecular modeling methods could provide directions on how to change the structure of photoswitchable ligands to obtain favorable wavelengths with the maintenance of the structural aspects necessary for molecule activation.

3. Solution of the problem

To investigate the possible relationship between the structure of potential photopharmaceutic and its ability to act in the expected mechanism computational model was chosen to optimize compounds of interest structures and reference molecules, consisting of platin-based already used drugs, including cisplatin. On optimized by ADF software [3] geometries, using the same computational program, energy decomposition analysis [4] was done to distinguish which energy contributions are mainly responsible for platin and ligands interaction. Performed calculations also show how structural changes caused by irradiation by specific wavelength, can impact these interactions. All obtained results were compared with data calculated for a group of reference molecules, which can give a hint of how the activity of new proposed platin complexes differs from that already used in therapies. The visualizations were made by using the adfview software to quantitatively show the charge transfer process occurring between metal and its ligands.

The typical geometry optimization jobs utilized 1 node with a duration of around 48h, while molecular dynamics jobs used 4-8 nodes (duration of approximately 50 days).

4. Conclusions

Described research provides some leads on how proposed structures can be advantageous over already existing compounds used as pharmaceuticals. It can also give directions for experimentalists on how to change the structure of the molecules to meet the assumptions of photopharmacology and cisplatin-based drug modeling more efficiently.

Acknowledgements. This research has been supported by NCN: OPUS grant (UMO-2021/41/B/NZ7/02484.). All calculations were possible through computing allocation on the Ares system at ACC Cyfronet AGH under the grants plgghb9 and plgghb10.

References

1. I. A. Riddell, and S. J. Lippard: Cisplatin and Oxaliplatin: Our Current Understanding of Their Actions. In Proc. Metal Ions Life Science, 2018.
2. W. A. Velema, W. Szymański, and B. L. Feringa: Photopharmacology: Beyond Proof of Principle. In Proc. Journal of The American Chemical Society, 2014.
3. Official SCM web site with information about ADF software: `https://www.scm.com/product/adf/`
4. L. Zhao, M. von Hopffgarten, D. M. Andrada, and G. Frenking: Energy Decomposition Analysis. In Proc. Wiley Periodicals, 2017.

Solvent Molecules Impact on the Nylon 6 Thermal Degradation Process: the Ab Initio Molecular Dynamics and DFT Study

Yuliia Didovets, Mateusz Z. Brela

Molecular Spectroscopy Group, Department of Physical Chemistry and Electrochemistry, Faculty of Chemistry, Jagiellonian University, Gronostajowa 2, 30-387 Kraków, Poland

yuliia.didovets@student.uj.edu.pl, brela@chemia.uj.edu.pl

Keywords: DFT, AIMD, nylon 6, polymer degradation process

1. Introduction

External conditions and the chemical environment are two key factors in reaction progress, important in the case of reaction investigation. However, these factors, especially solvation, should be analysed separately to describe their individual impact on the reaction progress. The explicit solvent model is frequently employed due to solvent molecules' capability to interact with the studied system. The solvent presence can drastically change the thermodynamics and kinetics (path and speed, respectively) of polymer degradation processes.

2 Description of the problem

Previously, the temperature effect, as well as the solvent presence treated implicitly, were included in the polymer degradation research of nylon 6 [1]. Obtained results proved the importance of both factors in the nylon 6 thermal degradation process. However, such a description of the system is incomplete. For this reason, solvent presence treated explicitly should be carefully studied in further research.

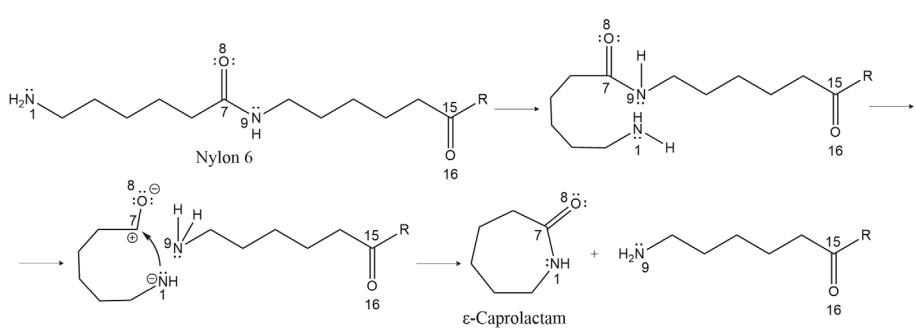

Fig. 1. Nylon 6 thermal degradation process scheme.

3. Solution of the problem

Computational models were constructed on the basis of previously optimized models [1]. Solvent molecules (water) were added to the computational model to account for two solvation shells.

CP2K software with Quickstep scheme [2] was used to perform ab initio molecular dynamics simulations. The NVT ensemble was chosen, and the Nosé-Hoover thermostat was used with the temperature set to 300 K. 1 fs timestep was applied, and the total simulation was ca. 50

ps. DFT method (BLYP-D3) and DZVP basis set with plane waves (cutoff 450 Ry) were used. For vibrational analysis, computational models were initially optimized in MOPAC software (PM7 semi-empirical method). Further geometry optimization was performed in ADF2019 software [3-4] using BP86-D3/TZP.

Approximately 2M computational hours on Ares supercomputer were used (plgghb10 grant). The typical molecular dynamics job utilized 8 nodes with 48 cores each, while geometry optimization jobs used 2 and 4 nodes.

4. Conclusions

Molecular dynamics results showed the formation of hydrogen bonds between the nylon 6 chain and water molecules. Further, water molecules were proved to assist in the nylon 6 thermal degradation process.

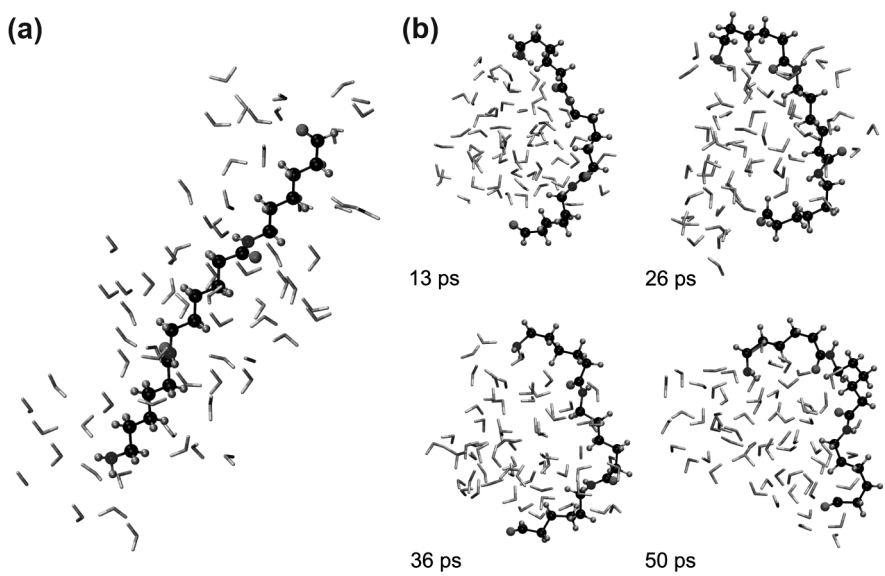

Fig. 2. Panel (a) shows the nylon 6 computational model structure; panel (b) shows snapshots of the computational model during the simulation.

Acknowledgements. This research was supported by grant IDUB/DigiWorld/2022/14 1027.0641.363.2019. The numerical experiments were possible through computing allocation on the Ares system at ACC Cyfronet AGH under the plgghb10 grant.

References

1. Y. Didovets and M. Z. Brela: “Theoretical Study on the Thermal Degradation Process of Nylon 6 and Polyhydroxybutyrate”, Physchem, 2022, 2, pp.334–346.
2. T. D. Kühne, M. Iannuzzi, et al.: “CP2K: An Electronic Structure and Molecular Dynamics Software Package - Quickstep: Efficient and Accurate Electronic Structure Calculations.” J Chem Phys, 2020, 152 (19), p.194103.
3. G. te Velde et al.: “Chemistry with ADF”, Journal of Computational Chemistry, 2001, 22, p.931.
4. ADF2019, SCM, Theoretical Chemistry, Vrije Universiteit, Amsterdam, The Netherlands, `http://www.scm.com`

Molecular Modeling of Selected Perovskites with Possible Application in Photovoltaics

Alicja Mikłas, Mateusz Z. Brela

Jagiellonian University, Faculty of Chemistry, Gronostajowa 2, 30-387 Kraków, Poland

alicja.miklas@doctoral.uj.edu.pl, mateusz.brela@uj.edu.pl

Keywords: perovskites, photovoltaics, band gap analysis, Density Functional Theory (DFT)

1. Introduction

Due to growing energy consumption, alternative sources of energy must be looked for. An extensively developed alternative energy source is photovoltaics. Nowadays, the most popular semiconductor used in photovoltaic (PV) cells is silicon. However, silicon-based PV cells have already reached their peak of efficiency. Alternative materials to replace silicon are being searched for. A group of materials that exhibit suitable physicochemical properties to replace silicon are perovskites [1].

Perovskites is a group of materials with the general formula ABX_3 where A stands for cation located in the vertex of the face-centered cubic lattice (e.g., Cs^+, $CH(CH_2)_2^+$), B for metal cation (e.g., Pb^{2+}, Sn^{2+}, etc.) and X for halogen anion (Cl^-, Br^-, I^- or coexistence of several halogens) placed in the core and apex of the octahedra, respectively. Two perovskites investigated for photovoltaics are $CsPbBr_3$ and $CsPbI_3$. However, $CsPbBr_3$ has too large a band gap value for PV applications, but shows good stability. $CsPbI_3$ shows a band gap value suitable for PV applications, but is highly unstable in PV cell operating conditions [2]. Hence, the goal is to synthesize perovskite with mixed halides, so bromine, and iodine with the general formula $CsPbBr_xI_{3-x}$.

2. Description of the problem

This work focuses on performing DFT calculations for perovskites that can be applied in photovoltaics. Investigated perovskites are $CsPbBr_3$, Cs,PbI_3 and perovskites with mixed bromine and iodine concentration with the general formula $CsPbBr_xI_{3-x}$. Regarding $CsPbBr_3$, it exists in three crystallographic polymorphs: cubic, orthorhombic, and tetragonal. All calculations were performed for all three polymorphs. $CsPbI_3$ exists in cubic and orthorhombic polymorphs, and all calculations were performed for both polymorphs.

The main part of the research is focused on calculating the influence of iodine and bromine concentration of investigated perovskite, on its unit cell parameters (a, b, c periods and unit cell volume V) and band gap value (E_g). Calculated values are also compared with experimental values of unit cell parameters and band gap measured for perovskites synthesized by PI during an internship in the Institute of Metallurgy and Materials Science Polish Academy of Science.

3. Solution of the problem

All $CsPbBr_3$ and $CsPbI_3$ polymorphs unit cell parameters and band gap values are calculated. Initial structures of $CsPbBr_3$ and $CsPbI_3$ were modified, and depending on the initial structure composition, halide was gradually substituted. In particular, if the initial structure is $CsPbBr_3$, bromine was gradually replaced with iodine to obtain perovskite with pure iodine $CsPbI_3$ according to the below path:

$$CsPbBr_3^* \rightarrow CsPbBr_2I \rightarrow CsPbBrI_2 \rightarrow CsPbI_3 \quad (1)$$

Path for $CsPbI_3$ as initial structure:

$$CsPbI_3^* \rightarrow CsPbBrI_2 \rightarrow CsPbBr_2I \rightarrow CsPbBr_3 \quad (2)$$

For both aforementioned paths, structures marked with a star (*) are initial structures from crystallographic measurements.

All calculations were performed in CP2K [3] with details: functional GGA: PBE (Perdew, Burke, Emzerhof, dispersive correction of vdW interactions D3-DFT Grimme, mixed wave base DZVP-MOLOPT-SR-GTH with plane waves and pseudopotential GTH-PBE.

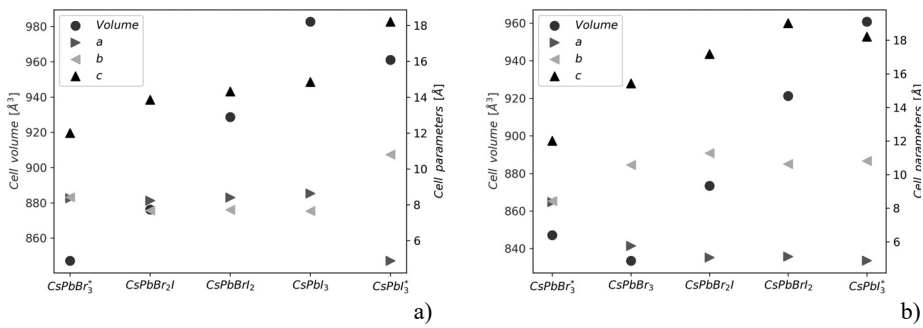

Fig. 1. Unit cell parameters for $CsPbBr_3$ orthorhombic: (a) $CsPbBr_3 \rightarrow CsPbI_3$; (b) $CsPbI_3 \rightarrow CsPbBr_3$.

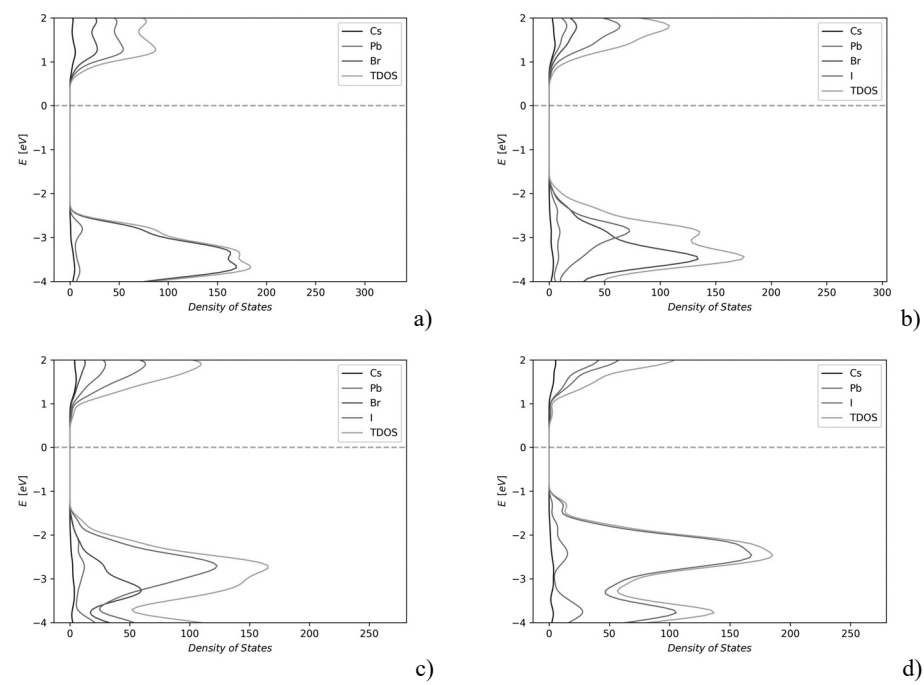

Fig. 2. Projected density of states (PDOS) for $CsPbBr_3 \rightarrow CsPbI_3$ orthorhombic for: (a) $CsPbBr^*_3$; (b) $CsPbBr_2I$; (c) $CsPbBrI_2$; (d) $CsPbI_3$.

4. Conclusions

The composition, as well as various concentrations of bromine and iodine in studied systems, influence unit cell parameters and band gap value. According to expectations, unit cell parameters increase with the increase of iodine concentration, and the band gap value decrease with the increase of iodine concentration. A similar trend was observed with experimental reference values measured from synthesized samples.

Acknowledgements. I would like to thank the Employees of the Institute of Metallurgy and Materials Science Polish Academy of Science for allowing me to perform the experimental study. This research was funded by the Priority Research Area Digiworld under the program Excellence Initiative – Research University at the Jagiellonian University in Kraków. The numerical experiment was possible through computing allocation on the Prometheus system at ACC Cyfronet AGH under the grant plghb8.

References

1. J. Zhang, G. Hodes, Z. Jin, L. Shengzhong: All-Inorganic CsPbX3 Perovskite Solar Cells: Progress and Prospects.; Angewandte Chemie International Edition, 2019, 58, 15596-15618.
2. D. Zhou, T. Zhou, Y. Tian, X. Zhu, Y. Tu: Solar Cells: Materials, Methods, and Future Perspectives; Perovskite-Based Journal of Nanomaterials, 2017.
3. T. D. Kühne, M. Iannuzzi, M. Del Ben, V. V. Rybkin, P. Seewald et al. CP2K: An electronic structure and molecular dynamics software package - Quickstep: Efficient and accurate electronic structure calculations, J. Chem. Phys. 152, 194103 (2020).

Computational Studies on Structural and Photophysical Properties of a 2,4-Dihydroxyphenyl-Substituted 1,3,4-Thiadiazole

Dominika Kaczmarczyk[1], Arkadiusz Matwijczuk[2], Monika Srebro-Hooper[1]

[1] Jagiellonian University, Faculty of Chemistry, Gronostajowa 2, 30-387 Kraków, Poland
[2] University of Life Sciences, Faculty of Environmental Biology, Akademicka 13, 20-950 Lublin

dominika.kaczmarczyk@doctoral.uj.edu.pl, arkadiusz.matwijczuk@up.lublin.pl, monika.srebro@uj.edu.pl

Keywords: Thiadiazoles, UV-Vis spectroscopy, Fluorescence spectroscopy, (TD)DFT calculations, Keto-enol tautomerism, Dual fluorescence, ESIPT, TICT

1. Introduction

The search for new antifungal drugs has become a matter of great importance for modern medicine, due to the increasing incidence of invasive fungal infections and resistance to antifungal agents [1]. In this context, 1,3,4-thiadiazole-based compounds, such as a thiadiazole-resorcinol hybrid NTBD (4-[5-(naphthalen-1-ylmethyl)-1,3,4-thiadiazol-2-yl]benzene-1, 3-diol, Fig. 1.) of confirmed antifungal activity [2,3], have recently gained considerable attention. Besides their biological activity, 1,3,4-thiadiazole derivatives also demonstrate a number of interesting spectroscopic, crystallographic and biophysical properties, which are often considered as relevant for pharmacological potential [4]. Importantly, a full rationalization of their experimental features, enabling an understanding of structure-properties relationships, can only be achieved with the help of quantum-chemical calculations.

2. Description of the problem

A detailed experimental spectroscopic characterization of NTBD revealed that in solvents with decreased medium polarity, e.g., n-hexane, and in DMSO/water [2] and methanol/water mixtures, this system exhibits an interesting emission feature, namely dual fluorescence. This phenomenon, produced by a single excitation, is usually explained in the literature by invoking effects such as excited-state intramolecular proton transfer (ESIPT), twisted intramolecular charge transfer (TICT), and processes related to aggregations (aggregation-induced emission (AIE) and aggregation-induced emission enhancement (AIEE)) [2]. Since assigning a proper origin is not a straightforward task, especially because the aforementioned effects may coincide, the main aim of our study was to understand the photophysics of NTBD based on quantum-chemical molecular modelling.

3. Solution of the problem

The calculations were performed using density functional theory (DFT), and its time-dependent variant (TDDFT) as implemented in the Gaussian 16 package, version C.01. Solvent effects (for methanol and water) were modelled via a polarizable continuum model (PCM). The systematic conformational analysis of NTBD in the ground state S_0, including various enolic and keto forms, was followed by calculations of the energy profile for the proton transfer (DFT-B3LYP+D3/6-311++G(d,p), DFT-B3LYP/aug-cc-pVDZ). In the next step, we modelled the UV-Vis spectra and fluorescence emission (via S_1 excited-state geometry optimizations). Subsequently, we computed energy profiles for ESIPT and TICT processes (TDDFT-B3LYP/aug-cc-pVDZ).

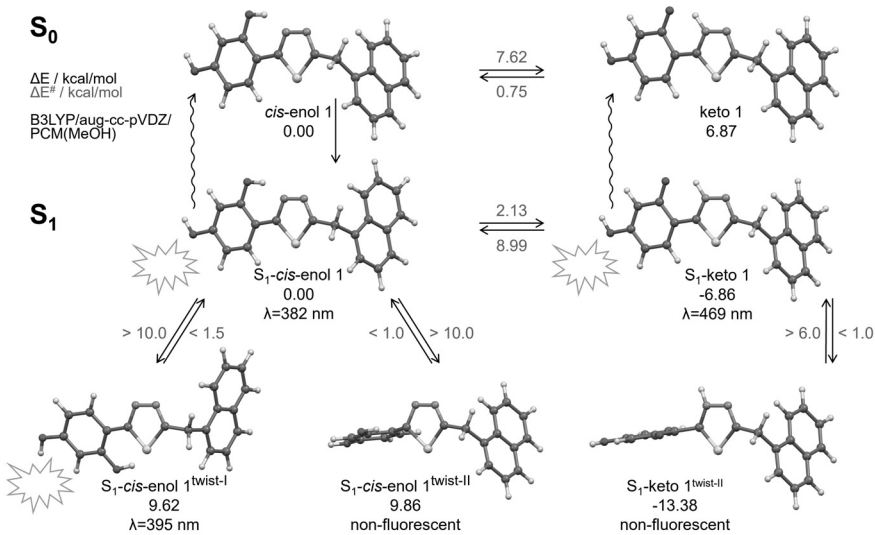

Fig. 1. Schematic representation of the photophysical processes for NTBD.

4. Results and conclusions

The results of the ground-state S_0 calculations demonstrated that in polar solvents, NTBD favorably adopts the enol form stabilized by the intramolecular hydrogen bond, i.e., *cis*-enol (Fig. 1.), and the presence of the keto isomer is unlikely. This was further supported by a very good agreement of the energetic position and shape of the UV-Vis spectra for *cis*-enol structures with the experiment. Conversely, in the excited state S_1 of NTBD, the keto isomer is considerably stabilized compared to its parent *cis*-enol, and, based on the calculated energy barriers for the ESIPT process, it can be concluded that *cis*-enol→keto tautomerization may indeed occur in S_1. Furthermore, as both isomers demonstrate different $S_1 \rightarrow S_0$ fluorescence vertical transition wavelengths, the one for enol (keto) agreeing well with the shorter-wavelength (longer-wavelength) band observed in the experimental emission spectra of this compound measured in methanol/water mixtures, the co-existence of the two tautomeric forms nicely explains the dual fluorescence effect seen for NTBD in such solutions. Finally, the intramolecular rotation of the resorcylic fragment relative to the 1,3,4-thiadiazole unit in S_1 (representing the TICT effect) was found to have a significantly high energetic barrier for the NTBD *cis*-enol, while for keto, it was essentially barrierless, with the corresponding twisted keto forms markedly stabilised and non-fluorescent. This highlights the important role of the aggregation effects present for NTBD in methanol/water mixtures (via enforcing planarity of the keto structures) in the occurrence of dual (enol- and keto-origin) fluorescence signals in such media and explains a single (enol-origin) emission band observed for NTBD in pure methanol.

Acknowledgements. This research has been supported by the PLGrid infrastructure: grant ID: plgcalcs4spect2022 (Prometheus) and plgphdqchem (Ares).

References

1. Revie NM., et al. Curr Opin Microbiol. 2018, 45, 70-76.
2. Dróżdż A., et al. Int J Mol Sci. 2023 24(4), 3430.
3. Budziak-Wieczorek I., et al. Sci Rep. 2022, 12(1), 22140.
4. Karcz D., et al. Int J Mol Sci. 2020, 21(16), 5735.

The Strategy of a Living Organism – the Simulation Model

Irena Roterman, Leszek Konieczny

Collegium Medicum – Jagiellonian University, Kraków, Poland

myroterma@cyf-kr.edu.pl, mbkoniec@cyf-kr.edu.pl

Keywords: systems biology, homeostasis, computer simulations in medicine

1. Introduction

The organization of functioning of the human body – the most complex system on our planet – is expected to be available for computer simulation. The availability of such system is not only the source of information as to the status of the system in a particular moment. It could be the tool for in silico experiments. The aim-oriented insertion of the local damage in activity may inform as to the nature of its consequences. The results of introduced damage of particular element may be local and limited to close neighborhood. Others – especially when based on communication disorder – may reveal the surprisingly long-distance consequences.

The model for computer simulation is presented. It may be applied to any living organism as well as to human body in particular. Such a tool is desperately expected for pathological processes recognition, especially for rare diseases.

2. Characteristics of the proposed system

The main characteristics of a living organism are:

1. The organism is the open system – many signals of chemical and of other characters are adopted by the living organism.
2. Despite of this opennes the organism is keeping the stability – called in biology – homeostasis. It is only one solution to satisfy these two conditions: the automatic control in the form of the network of negative feedback loops.

3. Model construction

The proposal to construct the system of mutual relations of negative feedback loops representing certain processes passing in the organism is presented.

The model is in contrast to other proposals basing on the structural unit which is one single protein. The structural-functional unit of the proteom construction in presented model is one negative feedback loop. The role of proteins participating in the activity of such loop is very well defined. This identification distinguishes the specificity of each role played by a particular protein like receptor or effector. Different number of proteins participates in one loop construction. It depends on the effector activity.

Two communication systems are proposed for loop-to-loop contacts and mutual influences. One of them is addressed to the effector, and the second one to the receptor. The first one is responsible for delivering the expected compound (the effector knows „How" to run a particular process), and the second – keeping the stable level of concentration – thus responsible for „How much?". Other proteins participation in the circle is the role of messenger for receptor-effector communication. Other proteins, participating in the one negative feedback loop construction, depend also on the necessary enhancement of the signal as well as the proteins responsible for transport – like membrane-anchored proteins' to transfer the signal molecules.

The number of protein engaged in one negative feedback loop construction depends mainly on the process performer by the effector. In case of effector activity in the form of cell division, the number of proteins engaged is quite large.

The signalisation addressed to the receptor is of the order character. It pushes the receptor to increase the level of stability in case of higher consumption of the product of a particular loop. This signal is as long active as long it reaches the receptor. In case of signal silencing, the loop goes back to standard parameters. The effector-addressed signal represents the form of more or less stable and permanent delivery of substrates.

4. Solution of the problem

The basis for the presented model is described in details in [1-4]. The test version for the limited number of units is available at `https://nfs.sano.science`, in which the user can model interconnected systems and their interactions, depending on system parameters – such as receptor sensitivity, effector reaction speed, or the time it takes for signals to travel between the receptor and the effector. This service allows performing the *in silico* experiment. The user may change arbitrarily the selected parameter receiving the feedback visualizing the system's characteristics in new, changed conditions, including total damage of the regulation system.

5. Conclusions

The model was tested by students of Medicinal Faculty Collegium Medicum – Jagiellonian University during the "Simulation in Medicine" course. Their comments may be taken into consideration for future work on the system.

Acknowledgements. This work/research has been supported allowing the numerical experiments what was possible through computing allocation on the Prometheus system at ACC Cyfronet AGH as part of the SANO project.

References

1. L. Konieczny, I. Roterman, P. Spolnik. Systems Biology – Functional strategies of living organism Springer 2014.
2. L. Konieczny, I. Roterman, P. Spolnik. Biologia Systemów – Strategia działania organizmu żywego – PWN 2021.
3. J. Wach, M. Bubak, P. Nowakowski, I. Roterman, L. Konieczny, K. Chłopaś. Negative feedback inhibition – Fundamental biological regulation in cells and organisms. In: Simulation in medicine – Pre-clinical and Clinical Applications. Ed: Irena Roterman-Konieczna, Walter de Gruyter GmbH, Berlin/Boston 2015, pp. 31-56.
4. L. Konieczny, I. Roterman, P. Spolnik. Systems Biology – Functional strategies of living organism – electronic version accessible in Internet – available soon.

Molecular Dynamics Simulations for the Michaelis Complex of Ectoine Synthase (EctC)

Justyna Andrys-Olek[1], Johann Heider[2], Tomasz Borowski[1]

[1] Jerzy Haber Institute of Catalysis and Surface Chemistry, Polish Academy of Sciences, 30-239 Kraków, Poland
[2] Department of Biology, Philipps-Universität Marburg, 35043 Marburg, Germany

{justyna.andrys, tomasz.borowski}@ikifp.edu.pl,
johann.heider@biologie.uni-marburg.de

Keywords: molecular dynamics simulation; ectoine synthase; metalloenzyme; near attack conformation; umbrella sampling; Michaelis complex

1. Introduction

Ectoine is a cell-protecting compound synthesised and used by bacteria to defend against osmotic stress [1]. The ultimate step of ectoine biosynthesis is catalysed by ectoine synthase enzyme (EctC), which requires iron ion for substrate binding and enzymatic catalysis. Despite the experimental studies on the enzyme, its structure-function dependency is not fully understood. The main goal of this study was to test existing hypotheses concerning EctC structural features and also to provide new insight into the formation of the EctC-substrate complex.

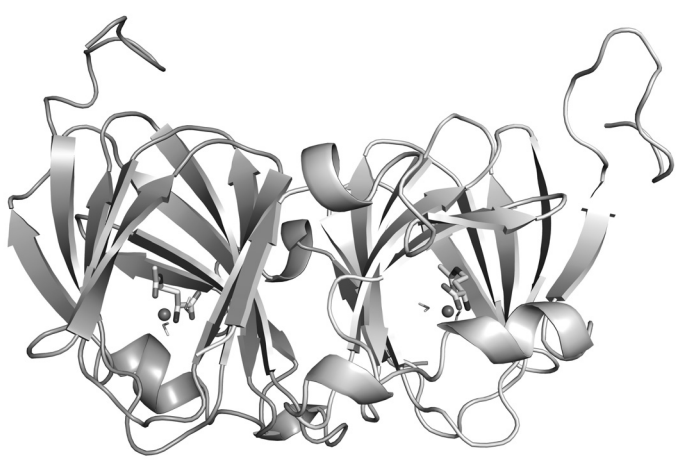

Fig. 1. Ectoine synthase dimer with both monomers occupied by substrate (N-γ-ADABA).

2. Description of the problem

Experimental studies on EctC [2,3] left some gaps concerning the formation of the Michaelis complex between EctC and the substrate (N-γ-ADABA):

1. Active site in a crystal structure for *P. Lautus* EctC—substrate complex (PDB: 5ONN) has weak electron density around Fe coordinates and Fe-ligands bonds are too long.
2. No data on protein-substrate complex dynamics.

3. No data on *P. Lautus* EctC in dimeric form.
4. Existence of two alternative Trp21 conformations in *P. Lautus* EctC Michaelis complex crystals.

3. Solution of the problem

The Amber 20 software was used to perform molecular dynamics (MD) simulations and potential mean force (PMF) calculations which are at the core of the study. We tested different dimer occupations and different geometries around Fe ion, substrate geometries and energetics of near-attack-conformation (NAC) formation in the substrate.

4. Conclusions

1. Six-coordinate geometry around Fe^{2+} ion is more plausible than four-coordinate.
2. Optimal arrangement of active site amino acids for Michaelis complex with the substrate in NAC conformation is required: (a) Arg25 strongly interacting with substrate carboxyl group; (b) Tyr52 interacts with substrate carboxyl group; (c) indole ring of Trp21 interacts with C4 atom in the substrate; (d) Ser23/Thr40 sporadically forms a hydrogen bond with the carboxyl group of the substrate.
3. Trp21 must be in „A" conformation that slightly dominates the occupancy in the crystal. Trp21 in "B" conformation can switch to "A" but not vice versa.
4. Binding of the substrate stabilises the α-II helical region, likely due to Arg25 involvement in N-γ-ADABA binding.

Acknowledgements. This research was supported in part by the PLGrid infrastructure. Computations were performed at Academic Computer Centre Cyfronet AGH under the grants: plgikbio21, plgikbio22.

References

1. Hermann, L.; Mais, C. N.; Czech, L.; Smits, S. H. J.; Bange, G.; Bremer, E. The Ups and Downs of Ectoine: Structural Enzymology of a Major Microbial Stress Protectant and Versatile Nutrient. Biol. Chem. 2020, 401, 1443–1468.
2. Czech, L.; Höppner, A.; Kobus, S.; Seubert, A.; Riclea, R.; Dickschat, J. S.; Heider, J.; Smits, S. H. J.; Bremer, E. Illuminating the Catalytic Core of Ectoine Synthase through Structural and Biochemical Analysis. Sci. Rep. 2019, 9, 364.
3. Widderich, N.; Kobus, S.; Höppner, A.; Riclea, R.; Seubert, A.; Dickschat, J. S.; Heider, J.; Smits, S. H. J.; Bremer, E. Biochemistry and Crystal Structure of Ectoine Synthase: A Metal-Containing Member of the Cupin Superfamily. PLoS ONE 2016, 11, e0151285.

Advances in the System for the Automatic Dogs' Skin Cancer Detection

Rafał Frączek[1,2], Michał Karwatowski[1,2], Jakub Grzeszczyk[1], Jakub Caputa[1], Piotr Pindel[1], Daria Łukasik[1], Maciej Wielgosz[1,2], Paweł Russek[1,2], Agnieszka Dąbrowska-Boruch[1,2], Ernest Jamro[1,2], Marcin Pietroń[1,2], Sebastian Koryciak[1,2], Kazimierz Wiatr[1,2]

[1] ACC Cyfronet AGH, Nawojki 11, 30-950 Kraków, Poland
[2] AGH University of Science and Technology, al. Mickiewicza 30, 30-059 Kraków, Poland

{rafalfr, mkarwat, wielgosz, russek, adabrow, jamro, pietron, koryciak, wiatr}@agh.edu.pl, {d.lukasik, j.grzeszczyk, j.caputa, p.pindel}@cyfronet.pl

Keywords: images, cytology, annotation, deep learning, cancer, skin

1. Introduction

In veterinary oncology, the speed and accuracy of diagnosis are crucial for the success of treatment. One way to achieve this is by using microscopic analysis of cytology samples, but only a limited number of doctors have the necessary training. Incorporating artificial intelligence into the diagnostic process can potentially improve the speed and accuracy of diagnoses.

2. Description of the problem

To develop a dependable AI model to aid physicians in the diagnostic process, a substantial dataset of annotated cytology images is required for training and testing. The task of thoroughly annotating these images manually can be quite labour-intensive due to the large quantity of both images and objects within each image that needs to be labelled. In addition, when the trained model is available, it is necessary to create a user-friendly web interface that can be used by doctors to interact with the model.

3. Solution of the problem

The originally developed system for the semi-automatic cytology images annotation has been presented in [1]. The initial version consists of several modules that are responsible for performing specific tasks in the process of medical image acquisition, annotation and artificial intelligence model training. As the result, the fine-tuned artificial intelligence model is obtained, which can be used to detect skin cancer cells on microscopic images.

The updated system includes new modules that enable a doctor to interact easily with the developed system. Also, underlying neural model has been updated, architecture continues to be based on CBNetV2 [2] backbone, with tuned parameters. The number of cell types that the model can recognize has been extended. As it is depicted in Fig. 1., the system consists of two paths that meet at the central point, which is the Ares supercomputer. The goal of the first path is to train the artificial intelligence model that will be utilised in the second path – the AI inference path used during diagnosis. Both training and inference procedures begin with the collection of a tissue sample from an animal. The sample is placed under the microscope, raw digital images are taken, and finally appended to the database. In the next step, only during the training procedures, a veterinary pathologist uses the developed GUI application to annotate the obtained images. Finally, the first path ends with training and deploying the model to the Ares supercomputer. For the second (inference) path, a doctor employees indirectly the model in the diagnosis procedure. The routine starts with a vet doctor who uses the developed web interface to submit a microscopic image for the automatic pathology detection. Through the web interface, the images are sent over the Internet connection to the web-service server, where they are processed by

the developed software module. The web server communicates with the Ares supercomputer, which hosts and executes (AI-inference) the trained artificial intelligence model for the cancer cells detection. Finally, the results are sent back to the web server, where the doctor can read the report that assists him in the diagnosis procedure.

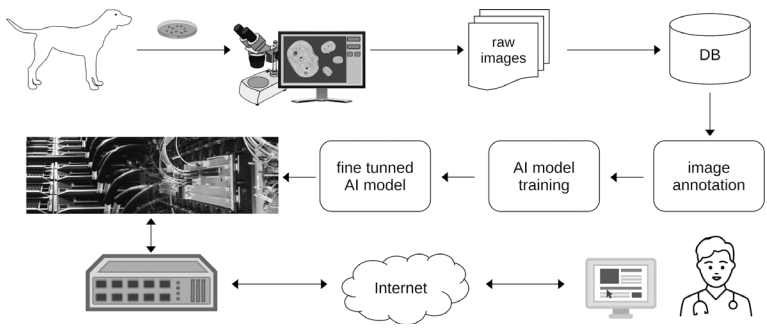

Fig. 1. The updated system flowchart.

An example of the recognition report is presented in Fig. 2. The report includes submitted by the doctor images on which the web-interface may draw rectangle marks over selected types of recognised cells.

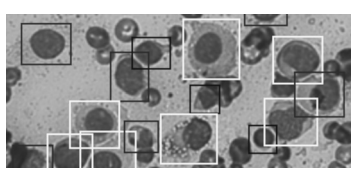

cell type	label	# cells
histiocytoma cell	histc	20
non-diagnostic	nondiag	20
lymphocyte	lymph	5

Fig. 2. An example of the recognition report.

4. Conclusions

The paper presents the advancements in the developed system for the automatic dogs' skin cancer detection. As compared to the previous system version, the new one can detect more cancer types with higher accuracy and provides a web user interface.

Acknowledgements. PLGrid grant ID: plglaoisi22/plglaoisi23. All models were trained on the PLGrid infrastructure. The complete training process of a single configuration takes about six hours using four NVIDIA V100 GPUs on the Ares server.

References

1. R. Frączek, M. Karwatowski, J, Grzeszczyk, J. Caputa, D. Łukasik, M. Wielgosz, P. Russek et al., A system for the fast and accurate cytology images annotation, KUKDM 2022: Fourteenth ACC Cyfronet AGH HPC Users' Conference, 7-8 April 2022: proceedings.
2. Liang T., Chu X., Liu Y., Wang Y., Tang Z., Chu W., Chen J., Ling H.: CB-NetV2: A Composite Backbone Network Architecture for Object Detection, 2021. URL: http://dx.doi.org/10.48550/arXiv.2107.00420

Sonochemical Formation of Fluorouracil Nanoparticles: Toward Controlled Drug Delivery from Polymeric Surfaces

Paulina Chytrosz-Wróbel[1], Monika Gołda-Cępa[1], Piotr Kubisiak[1], Waldemar Kulig[2], Łukasz Ćwiklik[3,4], Andrzej Kotarba[1]

[1] Faculty of Chemistry, Jagiellonian University in Krakow, Gronostajowa 2, 30-387 Kraków, Poland
[2] Department of Physics, University of Helsinki, P.O. Box 64, FI-00014 Helsinki, Finland
[3] J. Heyrovsky Institute of Physical Chemistry, Czech Academy of Sciences, Dolejskova 3, 18223 Prague, Czech Republic
[4] Institute of Organic Chemistry and Biochemistry of the Czech Academy of Sciences, Flemingovo nam. 542/2, CZ-16000 Prague 6, Czech Republic

paulina.chytrosz@doctoral.uj.edu.pl, mm.golda@uj.edu.pl, {kubisiak, kotarba@chemia.uj.edu.pl}, waldemar.kulig@helsinki.fi, lukasz.cwiklik@jh-inst.cas.cz

Keywords: drug nanoparticles, ultrasonic irradiation, cavitation bubble, nucleation mechanism, molecular dynamics

1. Introduction

The biomaterial surface can be substantially upgraded with the therapeutic function by the introduction of controlled, local elution of biologically active molecules [1]. The use of ultrasound for nanoparticles formation of controlled size and morphology has proved to be a simple, efficient, and eco-friendly method for compounds of varied chemical natures [2]. Molecular dynamics (MD) simulations have been widely used to study the details of biological processes occurring at biological interfaces [3].

2. Description of the problem

Sonochemical synthesis of nanoparticles is considered a complex process, where several steps are delineated. Therefore the exact mechanism of the nanoparticles formation assisted by ultrasounds is still unknown, hindering further advancement in drug delivery systems (DDS) based on the nanoparticles of bioactive molecules. However, progress can be stimulated by utilizing computational methods for molecular modeling. In particular, the atomistic MD simulations can probe the short length and time scale while fully accounting for the dynamics and molecular complexity of the formation of sonochemical nanoparticles.

3. Solution of the problem

In our study [4], we combined experiments and atomistic MD simulations to explore and optimize the mechanism of the sonochemically-assisted formation of fluorouracil nanoparticles. MD simulations were employed to gain molecular insight into the early stages of this process. The model systems with different ethanol concentrations in water and fluorouracil were constructed using the Packmol package.

All MD simulations were carried out using the GROMACS 2020.5 software. Force-field parameters of the fluorouracil and ethanol molecules were taken from the Amber ff99SB-ILDN, and the TIP3p water model was used. Periodic boundary conditions were employed in all dimensions. After construction, all systems were energy-minimized using the steepest descent algorithm to remove close contacts. Then the 200 ps equilibration using the NpT ensemble was performed, followed by production runs at the temperature of 310 K. The Nosé-Hoover thermostat, with a time constant of 0.5 ps, was employed to keep the temperature constant. The

Parrinello-Rahman barostat was used to keep the pressure at 1 bar with a time constant of 10 ps. The production run length for all simulations was 100 ns and was repeated 3 times.

4. Conclusions

We have successfully generated for the first time nanoparticles of fluorouracil, the bioactive molecule used in anticancer therapy. The formation of nanoparticles was stimulated by sonication of the fluorouracil–water–ethanol solution while optimizing the irradiation parameters to keep the drug's molecular structure intact. Fully atomistic molecular dynamics simulations were employed with a novel approach to model the cavitation bubbles and explain the mechanism of the formation of the nanoparticles at the molecular level. Combining experiments and computations can be used to conceptualise facile sonochemical synthesis of polymeric anti-cancer nanoparticle-based systems for the functionalization of esophageal stent covers.

Acknowledgements. This work/research has been supported by the Czech Science Foundation (22-27317K) and NCN (2021/03/Y/ST4/00071). The numerical experiment was possible through computing allocation on the Prometheus system at ACC Cyfronet AGH under the grants PLG/2021/014762, PLG/2021/014957 and PLG/2022/015495. The CPU-based MD simulations were running on 96 CPU cores and consumed approximately 8M normalized walltime hours. We wish to acknowledge the CSC – IT Center for Science (Espoo, Finland) for additional computational resources.

References

1. Qin, S. Y.; Zhang, A. Q.; Cheng, S. X.; Rong, L.; Zhang, X. Z. Drug self-delivery systems for cancer therapy Biomaterials Biomaterials 2017, 112, 234–247.
2. Liu, X.; Wu, Z.; Cavalli, R.; Cravotto, G. Preparation of Inorganic Nanoparticles and Nanocomposites for Drug Release-A Review Ind. Eng. Chem. Res. 2021, 60 (28), 10011–10032.
3. Enkavi, G.; Javanainen, M.; Kulig, W.; Róg, T.; Vattulainen, I. Multiscale Simulations of Biological Membranes: The Challenge To Understand Biological Phenomena in a Living Substance Chem. sRev. 2019, 119 (9), 5607–5774.
4. Chytrosz-Wrobel, P.; Golda-Cepa, M.; Kubisiak, P.; Kulig, W.; Cwiklik, L. and Kotarba A. Sonochemical Formation of Fluorouracil Nanoparticles: Toward Controlled Drug Delivery from Polymeric Surfaces ACS Applied Nano Materials Article ASAP DOI: 10.1021/acsanm.2c05332.

Computational Studies of Potential Mechanisms for Inhibiting the Toxicity of Amphotericin B via Molecular Association

Mikołaj Gurba[1], Arkadiusz Matwijczuk[2], James Hooper[1]

[1] Faculty of Chemistry of Jagiellonian University, Gronostajowa 2, Kraków, 30-387 Poland
[2] Department of Biophysics, University of Life Sciences in Lublin, Akademicka 13, Lublin, 20-950 Poland

mikolaj.gurba@student.uj.edu.pl, arkadiusz.matwijczuk@up.lublin.pl, james.hooper@uj.edu.pl

Keywords: docking site study, antifungals, Amphotericin B, DFTB, ETS-NOCV

1. Introduction

The threat to human health from fungal pathogens and infections is increasing. A recent WHO report established that the discovery and improvement of new and existing antifungal drugs are crucial [1]. Amphotericin B (AmB) is a well-known antifungal agent with excellent therapeutic effects, but also with a huge toxic effect [2].

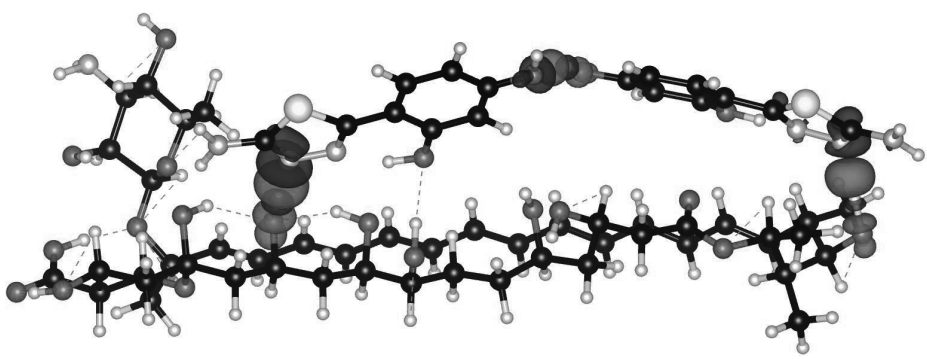

Fig. 1. Hydrogen bonds, visualized with the NOCV scheme, in one of the investigated systems.

2. Description of the problem

AmB usage in treating fungal diseases is limited because of its toxicity. Small molecules which contain thiadiazole components have been shown to reduce the toxicity of AmB. However the exact mechanism of this interaction remains unknown [3]. The goal of this project is to investigate the effects of thiadiazole derivatives on AmB aggregation with quantum chemistry methods.

3. Solution of the problem

The interaction between the thiadiazole derivatives and AmB molecules was investigated by first using a docking program (made “in-house”) to generate an initial pool of structures, then optimizing all of the generated structures with the DFTB suite provided via the ADF v.2021.103 software, and finally running complementary molecular dynamics and density functional theory

calculations (with the BLYP-D3 and B3LYP-D3 methods) [4]. The ETS-NOCV and NCI methods were used with selected structures in order to investigate the nature of the non-covalent interactions between AmB and the thiadiazole derivatives [5], [6]. The average size of systems considered in this study was around 150 atoms. Approximately 800 000 computational hours on both Prometheus (plgmedconformers grant) and Ares (plgmedconformers2022 grant) clusters were used.

4. Conclusions

The computational strategy of using a docking algorithm to generate a pool of geometries that were then fully optimized in (implicitly) solvated conditions at a semi-empirical density functional tight-binding level of theory provided insight into the existence of many locally stable structural motifs. All of the most stable motifs were those that created numerous hydrogen bonds (with large charge transfer components) between the thiadiazole derivatives and AmB. Importantly it was observed that the strength and character of the interactions change at higher concentrations of the thiadiazole derivative, and that the interaction can induce changes in the AmB molecule itself. This supports, in general terms, the premise that the presence of thiadiazole derivative can affect the aggregation of AmB in solution. The perspectives of this project include investigating other thiadiazole derivatives as well as implementing Machine Learning algorithms into binding site generation schemes of larger molecular clusters.

Acknowledgements. This research was funded by Polish National Science Centre grant 2019/35/B/NZ7/02756. The numerical experiment was possible through computing allocation on the Prometheus and Ares systems at ACC Cyfronet AGH under the grants plgmedconformers2022 and plgmedconformers. Arkadiusz Matwijczuk gratefully acknowledges the support from Kosciuszko Foundation, The American Centre of Polish Culture.

References

1. World Health Organization: WHO fungal priority pathogens list to guide research, development and public health action. World Health Organization, 2022.
2. A. Lemke, A. F. Kiderlen, and O. Kayser: Amphotericin B, Appl. Microbiol. Biotechnol., vol. 69, no. 2, 2005, pp.151-162.
3. B. Chudzik *et al.*: “Synergistic antifungal interactions of amphotericin B with 4-(5-methyl-1,3,4-thiadiazole-2-yl) benzene-1,3-diol”, Sci. Rep., vol. 9, no. 1, 2019, pp. 1-14.
4. R. Rüger *et al.*: *AMS DFTB 2019, SCM, Theoretical Chemistry*. Amsterdam, The Netherlands: Vrije Universiteit, 2019. [Online]. Available: `http://www.scm.com`
5. M. P. Mitoraj, A. Michalak, and T. Ziegler: “A Combined Charge and Energy Decomposition Scheme for Bond Analysis”, J. Chem. Theory Comput., vol. 5, no. 4, 2009, pp. 962-975.
6. E. R. Johnson, S. Keinan, P. Mori-Sánchez, J. Contreras-García, A. J. Cohen, and W. Yang: Simulation “Revealing noncovalent interactions”, J. Am. Chem. Soc., vol. 132, no. 18, 2010, pp. 6498-6506.

Hybrid-Kinetic Simulations of Quasi-perpendicular Shocks in High Beta Cosmic Plasmas

Stella Boula[1], Jacek Niemiec[1], Takanobu Amano[2]

[1] Institute of Nuclear Physics Polish Academy of Sciences, PL-31342 Kraków, Poland
[2] Department of Earth and Planetary Science, University of Tokyo, 7-3-1 Hongo, Bunkyo-ku, Tokyo 113-0033, Japan

stboula@ifj.edu.pl, jacek.niemiec@ifj.edu.pl, amano@eps.s.u-tokyo.ac.jp

Keywords: shock waves, electron acceleration, hybrid kinetic simulations, galaxy clusters

1. Introduction

We study particle acceleration at radio relics in galaxy clusters, which emit synchrotron radiation produced by non-thermal populations of electrons accelerated at so-called merger shocks. Low sonic Mach numbers and high plasma β conditions characterize these shocks. Here, we present an investigation of electron acceleration at merger shocks that develop multi-scale turbulence through plasma instabilities, including large-scale shock corrugations. We utilize a hybrid-kinetic numerical approach with a recently developed energetic particle-magnetohydrodynamic (EP-MHD) code [1].

2. Description of the problem

We perform 2D simulations in the (x-y) plane. A shock is created when an ion plasma beam moving along negative x-direction is reflected off the conductive wall at the left box boundary and interacts with the incoming plasma. The injected plasma carries a large-scale magnetic field, B_0, lying in the simulation plane at an angle θ_{Bn} to the shock normal. We study quasi-perpendicular shocks ($\theta_{Bn} > 45^o$) with sonic Mach number $M_s = u_{sh} / c_s$=2-4 (with u_{sh} the shock velocity and c_s the sound speed) in a range of plasma β, which is the ratio of thermal to magnetic pressure. We investigate the shock structure and critical Mach number at which Alfvén Ion Cyclotron (AIC) instability, responsible for the presence of shock surface ripples, is triggered by the ion temperature anisotropy at the shock, $Ti_\perp/Ti_\parallel > 1$, due to the shock-reflected ion component.

3. Numerical model and simulation setup

We use 3D numerical code [1] written in C++ with HDF5 file format and blitz++ libraries. The model assumes (i) collisionless quasi-neutral plasmas, (ii) kinetic particle species and fluids, and (iii) kinetic species dynamics governed by the Vlasov equation. Numerical schemes are (a) the PIC solver for kinetic species and (b) the Riemann solver for the fluid equations. The EP population interacts self-consistently with the MHD fluid. The code employs the exact form of the generalized Ohm's law.

About 150 simulations have been performed to scan the shock parameter space, such as the plasma β, the Mach numbers, and the angle θ_{Bn}. *The simulations produced ~500 TB of data and used a few million CPU hours.*

4. Results and conclusions

Fig. 1. shows 2D maps of electromagnetic shock structures (total magnetic field strength B_{tot}, B_z magnetic and E_y electric field components) for M_s=3. At this Mach number, the shocks are supercritical (see Fig. 2.), and through the reflected ion dynamics, they develop ion-scale fluc-

tuations in the shock ramp and downstream, which grow in the non-linear stage and cause shock front ripples. The observed shock structure in this stage is compatible with our recent results of fully kinetic 2D-PIC simulations [2]. The shock turbulence provides particle scattering in the particle acceleration processes at the shock.

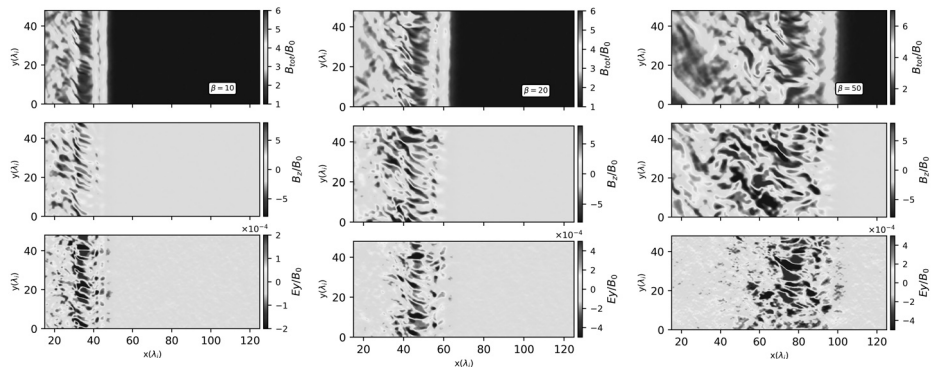

Fig. 1. Shock structure at the rippled stage at time t/Ω_{ci} = 15 for β = 10, 20 and 50, for M_s=3 and θ_{Bn} =75°. The turbulence structure weakly depends on plasma β.

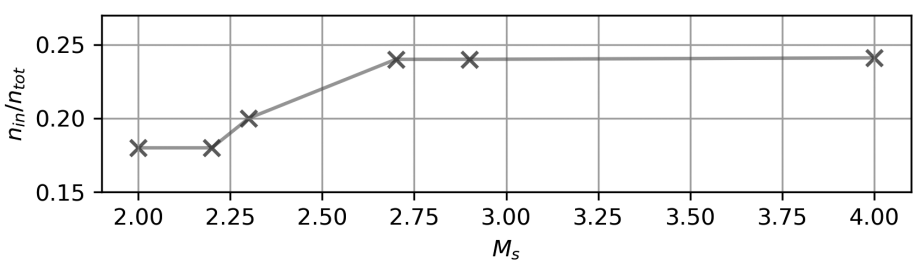

Fig. 2. Fraction of ions reflected from the shock as a function of shock sonic Mach number for simulations with β=20 and θ_{Bn} = 75°. Increased fraction translates into a higher $Ti_{\perp}/Ti_{\parallel}$ anisotropy that can trigger the AIC instability and the resulting shock rippling. The critical Mach number is between M_{cr}=2.3 and M_{cr}=2.7.

Acknowledgements. This work has been supported by Narodowe Centrum Nauki through research project 2019/33/B/ST9/02569. This research was supported by the PLGrid infrastructure through grants “astropic22” and “astropic23”.

References

1. T. Amano 2018, Journal of Computational Physics, 366:366.
2. O. Kobzar, J. Niemiec, T. Amano, et al. 2021, Astrophysical Journal, 919:97.

Particle-In-Cell Simulation of the Leptons Acceleration in the Precursor of Young Supernova Remnant Shock

Oleh Kobzar

Faculty of Computer Science and Telecommunication, Cracow University of Technology,
ul. Warszawska 24, 31-155 Kraków, Poland

oleh.kobzar@pk.edu.pl

Keywords: cosmic rays, electrons, positrons, electromagnetic turbulence, PIC simulations

1. Introduction

Energy spectra of the Galactic cosmic rays (CR) are close to the simple power-law distribution with maximum energies of ~ 2 PeV for hadronic and ~ 1 TeV for leptonic components. The last observations of the CR leptons indicated their deviation from the typical simple power-law with excesses for the electrons at 0.1 – 1 TeV, and much harder positron spectra at 20 – 200 GeV [1]. These results are important for understanding the physics of the CR sources. Here we check the assumption, that electromagnetic turbulence acting in the vicinity of supernova remnant shock may be responsible for these effects.

2. Particle-In-Cell simulations as a key solution

Since the considered systems are strongly nonlinear, they can be studied with numerical methods, requiring extremely large computational resources utilized with high-performance codes. We used Particle-In-Cell (PIC) simulations, a self-consistent first-principle method for collisionless plasma. It follows the individual particles and solves Maxwell's equations for the electromagnetic fields on a spatial grid. The simulations have been realized with the use of advanced MPI-based parallel relativistic code TRISTAN [2]. The code has been rewritten in FORTRAN90 and modified to use the HDF5 file format libraries and improved algorithm of the particle sorting [3]. Due to these changes, general performance has been increased up to ~ 30%. Due to the HDF5 format of the output files, the data post-processing has also been sped up.

3. Setup of simulation and results

The 2D-3V PIC-simulation has been performed in the rectangular computational box of 6000 x 2400 cells, containing 9 macro-particles per cell for each specie (i, e^-, e^+, CR), totally 518.4 mln particles. The periodic boundary conditions were applied in all directions. We used 240 CPU cores on 10 nodes, totally about 50 000 CPU-hours and 2 TB of disk space. In order to fit in the available computational resources in reasonable space and time limits, the reduced ion-to-electron mass ratio $m_i/m_e = 50$ has been used instead of realistic.

The simulated physical conditions were typical for the precursor of a young supernova remnant. We assume the pre-existing small population of positrons (10% of the electron amount). The cosmic ray (CR) particles, being previously accelerated at the shock, drift through the upstream plasma and generate the electromagnetic turbulence through the non-resonant Bell's instability [4], as shown in Fig. 1 (a). In turn, these waves interact with particles, resulting in their significant heating. The evolution of energy spectra is also shown in Fig. 1. for ions (b), electrons (c) and positrons (d). One can note that the energy of all particles increases sufficiently. Panels (e) and (f) in Fig. 1. show the growth of the particle average kinetic energy, measured in units of the electron rest energy, and their maximum relativistic Lorentz-factor, correspondingly. There is an obvious correlation between heating processes and electromagnetic turbulence.

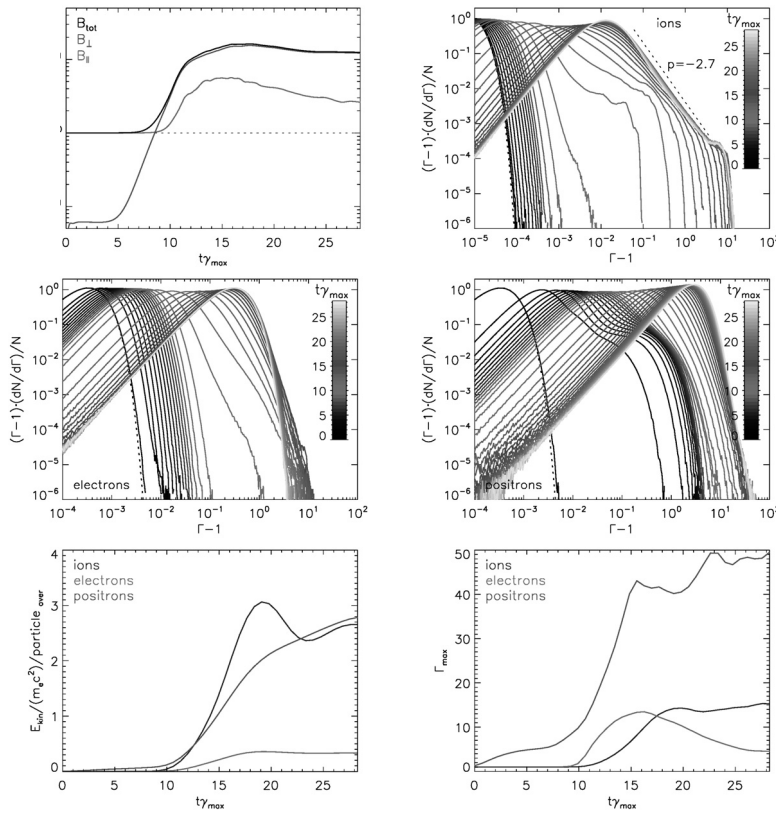

Fig. 1. Time evolution of the system: growth of the magnetic turbulence (a); evolution of energy spectra for ions (b), electrons (c) and positrons (d); growth of the average particle kinetic energy (e), and maximum relativistic Lorentz-factor (f) for ions (*dark-blue*), electrons (*green*) and positrons (*red*).

4. Conclusions

The CR-driven electromagnetic turbulence generated through non-resonant Bell's instability has been found to facilitate the efficient heating of the background plasma. Second order Fermi processes lead to stochastic scattering of plasma ions. Ambient electrons remain close to the bulk equilibrium with ions, being largely thermalized. Positrons are heated much more efficiently than electrons. The achieved positron energies are comparable with those of ions, which could be enough for injection to DSA. Therefore the lepton (pre-)acceleration is found to be strongly charge-dependent, in agreement with recent observational data.

Acknowledgements. The numerical experiment was possible through computing allocation on the Prometheus system at ACC Cyfronet AGH under the grants "astropic21" and "astropic22".

References

1. Z. L. Weng, V. Vagelli, AMS Collaboration. Nuclear and Particle Physics Proceedings. v. 273–275, April–June 2016, p. 466–472.
2. J. Niemiec, M. Pohl, T. Stroman, K.-I. Nishikawa, 2008, Astrophys. J., v. 684, p. 1174.
3. A. Dorobisz, M. Kotwica, J. Niemiec, O. Kobzar, A. Bohdan, K. Wiatr, 2018, LNSC, 10777, p. 156.
4. O. Kobzar, J. Niemiec, M. Pohl, A. Bohdan, 2017, Mon. Not. R. Astron. Soc, v. 469, p. 4985–4998.

Differences Between Vibrational Wavepackets Generated via Singlet Fission and Those Shaped by Direct Raman Pumping

Grzegorz Mazur[1], Marcin Andrzejak[1], Tomasz Skóra[2], Piotr Petelenz[1]

[1] Faculty of Chemistry, Jagiellonian University, ul. Gronostajowa 2, 30-387 Kraków, Poland
[2] Scientific Computing and Imaging Institute, University of Utah , 72 Central Campus Drive, Salt Lake City, UT 84112, US

{mazur, andrzeja, petelenz}@chemia.uj.edu.pl, tskora@ichf.edu.pl

Keywords: singlet fission, pump-probe spectroscopy

1. Introduction

Singlet fission [1] recently regained significant interest owing to its promise to increase the efficiency of photovoltaic devices [2]. To achieve this goal, a thorough understanding of the physical mechanisms of singlet exciton fission is necessary. One of the experimental techniques employed is the femtosecond Pump-Probe Spectroscopy (fsPPS) [3]. However, the theoretical model underlying the experiment's interpretation may contain some loopholes, which can result in incorrect physical conclusions.

2. Description of the problem

Specifically, it was suggested in the literature that comparison of fsPPS of the vibrational coherences generated in the triplet-pair electronic state via singlet fission with those in which coherences were shaped independently by direct Raman scattering might explain the role of individual vibrational modes in the fission process [4].

3. Solution of the problem

We demonstrate that there is no reason to expect the spectra to coincide. Our claim is based on the fact that the vibrational wavepackets generated in the two types of experiment are formed by different mechanisms, with different dependence on the light wave electric field and Franck-Condon integrals.

The problem is illustrated in the example of 13,13'-bis(mesityl)-6,6'-dipentacenyl (DPMes) [4]. Using quantum-chemical calculations to obtain the values of the respective Franck-Condon integrals and a simple model [5], we show that one of the main factors determining the form of the vibrational wavepackets generated in the considered experiments is the energy profiles of the pumping laser.

4. Conclusions

We demonstrate that if the pumping laser profile is neglected, the comparison of the generated vibrational coherences may lead to confusing interpretation.

Acknowledgements. The quantum-chemical calculations were possible through computing allocation on the Prometheus system at ACC Cyfronet AGH under the grants plgvibfission and plgvibfission2.

References

1. Smith, M. B.; Michl J. Singlet fission. Chem Rev. 2010;110:6891–6936.

2. Rao, A., Friend, R. H. Harnessing singlet exciton fission to break the Shockley–Queisser limit. Nat. Rev. Mater. 2017;2:17063.
3. Kim, W.; Musser, A. J. Tracking ultrafast reactions in organic materials through vibrational coherence: vibronic coupling mechanisms in singlet fission. Advances in Physics: X, 6:1, 1918022.
4. Schnedermann, C.; Alvertis, A. M.; Wende T.; et al. A molecular movie of ultrafast singlet fission. Nat Commun. 2019;10:4207.
5. Andrzejak, M.; Skóra, T.; Petelenz, P. Is Vibrational Coherence a Byproduct of Singlet Exciton Fission? J. Phys. Chem. C 2019, 123, 91-101.

Particle Transport Simulation for the Personalized Radiotherapy

Leszek Grzanka[1,2,3], Szymon Kania[1,2], Jakub Niechaj[1,2], Łukasz Pitrus[1,2]

[1] AGH University of Science and Technology, al. Mickiewicza 30, 30-059 Kraków, Poland
[2] ACC Cyfronet AGH, Nawojki 11, 30-950 Kraków, Poland
[3] Institute of Nuclear Physics Polish Academy of Sciences, Radzikowskiego 152, 31-342 Kraków, Poland

grzanka@agh.edu.pl, {kania, niechaj, pitrus}@student.agh.edu.pl

Keywords: particle transport simulations, treatment planning, radiotherapy

1. Introduction

Particle transport simulations are a crucial tool in the development of treatment plans for hadron and classical therapy. Monte-Carlo methods have been widely used for their ability to accurately model particle interactions and transport in complex geometries. Massively parallel simulations utilizing high-performance computing resources can reduce the turnaround time for treatment planning. Modelling of particle interactions boosts the research of state-of-the-art treatment techniques.

2. Description of the problem

Particle transport simulations require significant computing resources, particularly for complex treatment planning scenarios. However, the utilization of High-Performance Computing (HPC) resources can be challenging for many researchers and clinicians who may not have the necessary expertise or access to the required infrastructure. To address this challenge, we propose a user-friendly web interface that simplifies the access and utilization of HPC resources for particle transport simulations.

3. Solution of the problem

We designed and implemented a platform aiding simulations for personalized medicine. It consists of a web interface capable of defining simulation parameters, driving its execution, and visualizing the results. Application backend supports execution of parallel jobs on HPC resources equipped with SLURM workload manager. The simulation engine, SHIELD-HIT12A code [1], provides accurate models for particle interaction with matter. The demo version and source code of the application is freely available on a GitHub platform.

4. Conclusions

The yaptide platform was applied to model treatment plans used in experiments conducted at Aarhus University. The development version of the platform was deployed in the C3 cloud PLGrid infrastructure and utilised the resources of the Ares supercomputer.

Acknowledgements. This work has been supported by EuroHPC PL Project, Smart Growth Operational Programme 4.2. The numerical experiment was possible through computing allocation on the Ares system at ACC Cyfronet under the grants plgccbmc11 and plgyaptide2.

References

1. Bassler, Niels, et al. „SHIELD-HIT12A-a Monte Carlo particle transport program for ion therapy research." Journal of Physics: Conference Series. Vol. 489. No. 1. IOP Publishing, 2014.

Improving Hip Dysplasia Diagnosis in Dogs through Augmented 3D Video Simulation

Krystian Strzałka[1], Szymon Mazurek[1], Maciej Wielgosz[1,2], Jakub Caputa[1], Rafał Frączek[1,2], Michał Karwatowski[1,2], Jakub Grzeszczyk[1], Jan Krupiński[1], Daria Łukasik[1], Anna Śmiech[3], Paweł Russek[1,2], Agnieszka Dąbrowska-Boruch[1,2], Ernest Jamro[1,2], Marcin Pietroń[1,2], Sebastian Koryciak[1,2], Kazimierz Wiatr[1,2]

[1] ACC Cyfronet AGH, Nawojki 11, 30-950 Kraków, Poland
[2] AGH University of Science and Technology, al. Mickiewicza 30, 30-059 Kraków, Poland
[3] University of Life Sciences, al. Akademicka 13, 20-950 Lublin, Poland

k.strzalka@cyfronet.pl,
anna.smiech@up.lublin.pl, {rafalfr, mkarwat, wielgosz, russek, adabrow, jamro, pietron, koryciak, wiatr}@agh.edu.pl,
{s.mazurek, j.krupinski, d.lukasik, j.grzeszczyk, j.caputa}@cyfronet.pl

Keywords: dog hip dysplasia, deep learning, graph neural network, computational veterinary medicine

1. Introduction

Hip dysplasia in dogs is a genetic disorder that results in underdeveloped hip joints, leading to joint instability and degeneration over time. To diagnose hip dysplasia, a combination of physical examination and X-rays is usually required, both of which require specialised diagnostic equipment and trained professionals. Our goal is to develop a robust and lightweight pipeline that can classify a dog's gait based on video footage. Due to the low data availability, data augmentation in the form of 3D video simulation is required. This simulation will be incorporated into the examination pipeline depicted in Fig. 1.

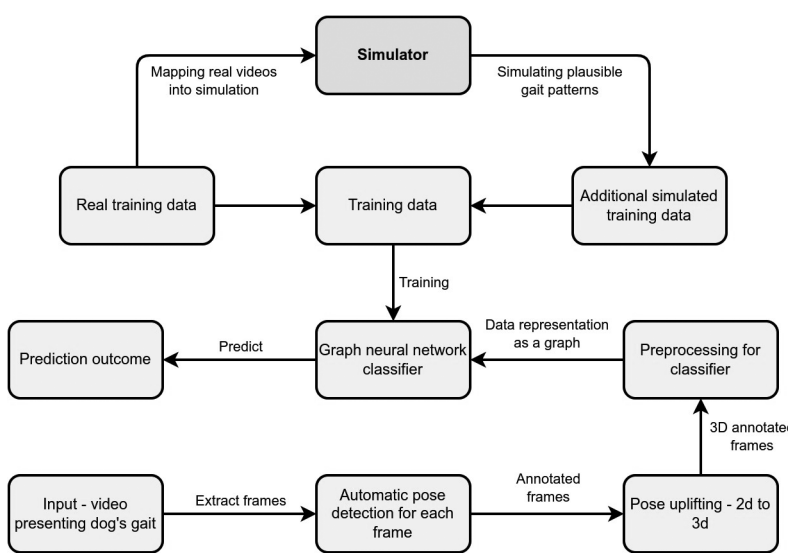

Fig. 1. Overview of the whole diagnostic system that this work is a part of.

2. Description of the problem

The generation of synthetic data is a critical aspect in training pipeline elements such as pose detection, pose uplifting, and classifiers. The availability of high-quality synthetic data is essential for developing accurate and robust models, particularly when real-world data is scarce or challenging to acquire. In order to train the aforementioned models, the data must include videos, 2D pose data, 3D pose data, joint visibility data, and a binary label indicating whether the gait is abnormal or healthy. Each of these data parameters plays a crucial role in the performance of the models, allowing them to learn and identify key patterns and features that differentiate between healthy and abnormal gaits.

3. Solution of the problem

The videos were generated using Blender 3.3 [1] Python API, using Blenderproc [2] library. Scenes created in the simulation are randomised in terms of camera position, lighting, and objects visible in the scene. Dog mesh with either healthy or unhealthy gait animations is loaded into the scene, providing a binary label. Scenes are randomly populated with a set of HDRis and meshes from polyhaven.com. Simulation provides all data required for pipeline training. The simulation output is shown in Fig. 2.

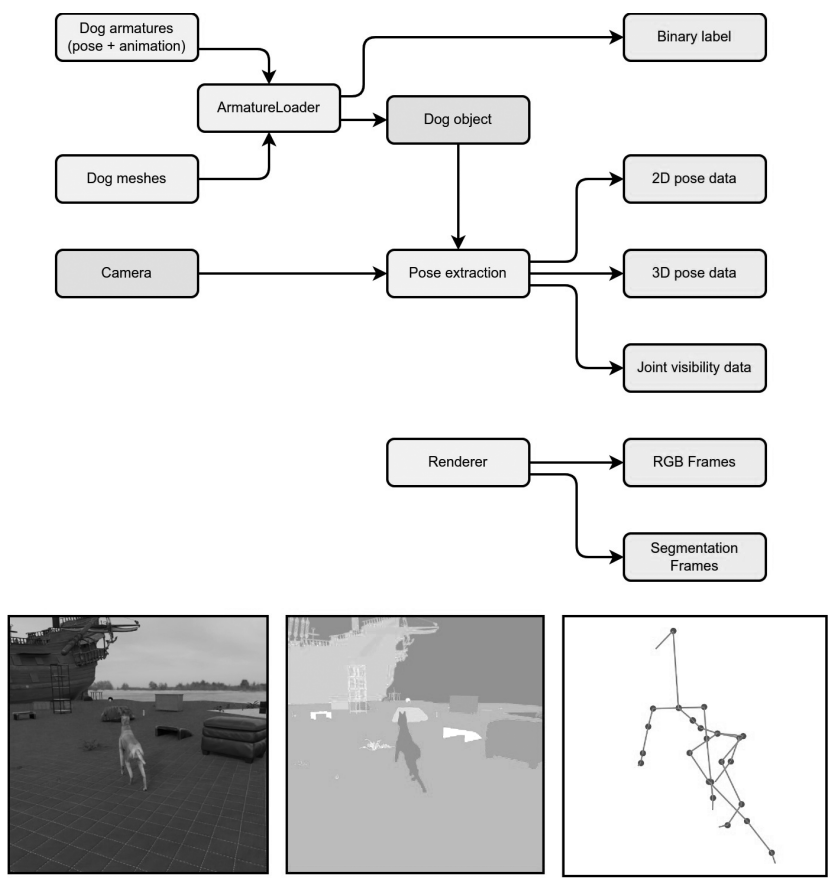

Fig. 2. Overview of the simulation with an example of its output.

4. Conclusions

The data generated from simulations are valuable resources that can be further enhanced by incorporating additional meshes and animations collected from real-world data sources. By generating various combinations of gaits and meshes in random environments, a large dataset can be obtained. Access to a large data set can greatly improve the accuracy and performance of machine learning models. This is because the models can learn from a wider range of samples and make more informed decisions.

Acknowledgements. PLGrid grant ID: plglaoisi23.

References

1. B. O. Community, Blender – a 3D modelling and rendering package. Stichting Blender Foundation, Amsterdam: Blender Foundation, 2018. [Online]. Available: `http://www.blender.org`
2. M. Denninger et al., "BlenderProc2: A Procedural Pipeline for PhotorealisticRendering", JOSS, vol. 8, no. 82, p. 4901, Feb. 2023, doi: 10.21105/joss.04901.

Development of the Machine Learning Based Track Reconstruction in the MUonE Experiment

Miłosz Zdybał, Marcin Kucharczyk, Marcin Wolter

Institute of Nuclear Physics Polish Academy of Sciences, Radzikowskiego 152, 31-342 Kraków, Poland

{milosz.zdybal, marcin.kucharczyk, marcin.wolter}@ifj.edu.pl

Keywords: machine learning, artificial neural networks, track reconstruction, high energy physics

1. Introduction

In a world where high-energy physics experiments produce ever larger amounts of data, new methods of fast and efficient track reconstruction are needed to handle the immense load. Storing the unprocessed data is not feasible, forcing experiments to process events online (before saving them on disks) using algorithms of quality similar to ones used previously in the offline analysis, without time constraints. The MUonE experiment [1] performs trials of the application of machine learning based algorithms to address this problem.

2. Description of the problem

The MUonE's tracking system is designed to precisely measure the scattering angles of the outgoing muon and electron in the $\mu e \rightarrow \mu e$ elastic process. It consists of 40 tracking stations with a target and three layers of the tracking modules, each built of two layers of silicon strip sensors. Each of the registered hits is represented with two coordinates, one read from the sensor, the other one being the sensor position along the beam. The goal of the reconstruction algorithm is to provide parameters of 3D tracks of outgoing particles.

3. Solution of the problem

The evolution of the machine learning based track reconstruction algorithm for the MUonE experiment will be presented, in particular, machine learning based pattern recognition in 3D. From the first attempts based on convolutional neural network in 2D [2], through the initial deep neural network based approach to the latest results, which reconstruction is performed in 3D. Perspectives of applying graph neural networks will be discussed.

4. Conclusions

In the trials using simulated data samples corresponding to the Test Beam 2018 and the Test Run 2022, it was shown that a solution based on artificial neural networks can compete with the classical solution in terms of reconstruction efficiency and precision. Additionally, improvement in the execution time can be achieved at the level of pattern recognition by replacing CPU-intensive iterative algorithm with neural network returning result in a single iteration.

Acknowledgements. The numerical experiment was possible through computing allocation on the Prometheus system at ACC Cyfronet AGH under the grants plgflav and plglhcbqee.

References

1. G. Abbiendi et al.: "Letter of Intent: the MUonE project", 2019: https://cds.cern.ch/record/2677471
2. M. Kucharczyk, M. Wolter: „Track Finding with Deep Neural Networks", in: Computer Science 20.4, 2019.

Deep Neural Networks for the Calibration of Timing Detectors

Mateusz Kocot[1], Krzysztof Misan[1], Valentina Avati[1], Edoardo Bossini[2], Leszek Grzanka[1], Nicola Minafra[3]

[1] AGH University of Science and Technology, al. Mickiewicza 30, 30-059 Kraków, Poland
[2] INFN Sezione di Pisa, Pisa, Italy
[3] Department of Physics and Astronomy, University of Kansas, Lawrence, KS, United States

{kocot, misan}@student.agh.edu.pl, grzanka@agh.edu.pl,
{valentina.avati, edoardo.bossini, nicola.minafra}@cern.ch

Keywords: deep neural networks, timing detectors, diamond sensors, CERN, PPS

1. Introduction

The Precision Proton Spectrometer (PPS) at the CERN's LHC performs timing measurements with the targeted precision of the order of picoseconds. Diamond-made sensors are inserted into the LHC beam pipes at the distance of approx. 200 m from the place where the particle collisions occur. One of the goals is measuring the arrival timestamps of 'scattered' protons whose trajectory is slightly divergent from the beam. A particle flying through the sensor causes a peak in the registered voltage.

2. Description of the problem

The PPS timing system produces sampled time series of voltage. The state-of-the-art method – Constant Fraction Discriminator – computes particle timestamps by normalising the amplitudes of the voltage signals and establishing a fixed threshold. This solution alleviates the effects of the so-called time walk effect stemming from amplitude differences. However, it is prone to errors resulting from the noise present in the data. It is also considering a limited number of voltage samples.

3. Solution of the problem

Deep neural networks achieve promising results in the field of time series analysis, including the prediction of a particle's time of arrival. The most popular approaches involve convolutional architectures, mainly based on UNet (e.g. [1]). We tested several architectures, including the multilayer perceptron (MLP), a convolutional network based on VGG and UNet. The networks were implemented in Python, using the TensorFlow library. We used a PC with an RTX 3070 GPU for preliminary experiments with the networks. For final hyperparameter tuning, the Ares supercomputer was used.

4. Conclusions

We were able to improve the timing precision of the state-of-the-art method. The improvements ranged from 9% to 23%, depending on the detector's readout channel. The best precisions were obtained using the UNet-based networks, which outperformed classical convolutional architectures and MLP.

Acknowledgements. The project was funded by the Polish Ministry of Education and Science, project 2022/WK/14. The numerical experiment was possible through computing allocation on the Ares system at ACC Cyfronet AGH under the grant plgccbmc11.

References

1. Eric Berg, Simon R Cherry. “Using convolutional neural networks to estimate time-of-flight from PET detector waveforms”. Physics in Medicine & Biology 63.2 (2018) p. 104005.

Neural Networks for the Analysis of Particle Tracing in PIC Simulations

Gabriel Torralba Paz[1], Artem Bohdan[2], Jacek Niemiec[1]

[1] Institute of Nuclear Physics Polish Academy of Sciences, Radzikowskiego 152, 31-342 Kraków, Poland
[2] Max-Planck-Institut für Plasmaphysik, Boltzmannstr. 2, DE-85748 Garching, Germany

gtorralba@ifj.edu.pl, artem.bohdan@ipp.mpg.de, jacek.niemiec@ifj.edu.pl

Keywords: neural networks, kinetic plasma simulations, particle tracing, Buneman instability

1. Introduction

We study cosmic ray acceleration processes at astrophysical shocks by using Particle-In-Cell (PIC) plasma simulations. A powerful technique to analyse these mechanisms is by tracing individual particles. However, the by-eye inspection of particle trajectories includes a high level of bias and uncertainty, and pinpointing the specific acceleration mechanisms is very difficult. Therefore, we propose the use of neural networks (NNs) to speed up the analysis and lower the bias in our analysis. The dataset consists of 210,000 particles, for which we have traced the three components of particle momenta as time series of 1200 time steps long. The particles are taken from our recent PIC simulations of non-relativistic shocks, in which the Buneman instability pre-accelerates electrons to high energies in the shock upstream. We perform regression and anomaly detection on the dataset by using a Convolutional NN. The proposed methodology may considerably simplify particle classification in large-scale PIC and hybrid kinetic simulations.

2. Description of the problem

Electrons in our dataset have been energized by the Buneman instability [1], that operates upstream of quasi-perpendicular high Mach number shocks and generates large-amplitude electrostatic waves that accelerate electrons via the so-called Shock Surfing Acceleration process. In our PIC simulations, we traced 210,000 particles and recorded their momenta over 1,200-time steps. Besides the momentum data, we compute for each particle a label representing the maximum kinetic energy achieved by the particle. Only a small fraction of the particles that pass through the region dominated by the Buneman instability is accelerated. This gives an imbalanced dataset consisting of two populations: thermal non-energetic electrons and the energetic electrons that form a non-thermal tail in all-electron spectra. Analysing such a huge dataset cannot be done by using visual inspection or any relatively simple human-designable criteria.

3. Solution of the problem

We use neural networks to tackle the problem of dealing with very large datasets and obtain a better precision of the classification than just a simple by-eye inspection. We perform regression and anomaly detection by using a Convolutional NN (CNN) and a CNN auto-encoder, respectively. To build the neural networks, we use Keras, a high-level API for development of neural networks built in Python. As the required amount of memory and computational power to train these neural networks is large, we use Ares and Athena clusters installed at Cyfronet to perform our calculations. To train and test our models we use 8 Tesla V100-SXM2 GPUs from the plgrid-gpu-v100 partition and cuDNN library from NVIDIA, necessary for deep learning calculations on GPUs. The size of the datasets is 20 GB in total, and the training may take around 40-50 minutes for regression and 1 hour and 30 minutes for anomaly detection.

We compare the true maximum kinetic energy (from the dataset) and the predicted value computed by the NN for regression. To counter the imbalance in the data, we apply sample weights [2] to the dataset as well as transform the dataset to log scale to flatten the histogram and thus obtain a more balanced dataset. We obtain a linear regression $y = 1.0050(\pm 0.0005)\, x + 0.0212(\pm 0.0015)$ with an $R^2 = 0.9892$, which is an excellent result for a very noisy and imbalanced data we use.

The anomaly detection, an unsupervised algorithm, compares the input time series with a reconstruction of the time series after going through the auto-encoder. If a reconstructed particle trajectory does not resemble the original, it means that that particle is an anomaly. In our dataset such particles represent the minority in all particle population (non-thermal particles). We label particles as energetic if their maximum Lorentz factor γ is greater than 1.1. Table 1 shows the results of the neural network. The more diagonal the table is, the better results we have. Out of 1200 energetic particles, 642 of them were predicted correctly, giving a ratio of 0.535. The anomaly detection precision is thus lower than that of the regression. Note, however, that particle labels are not used in this case and the NN is still able to discern correctly between energetic and non-energetic particles. Out of 648 particles that are predicted as anomalies, only 6 of them are non-anomalies, giving a ratio of 0.99. This can be summarised as follows: There are 1200 energetic particles, and we obtain 648 anomalies. 99% of the anomalies are true anomalies (642), which means that 46.5% of anomalies are missing.

Tab. 1. Anomaly detection results.

	True Anomaly	True Non-anomaly
Predicted Anomaly	642	6
Predicted Non-anomaly	558	61794

4. Conclusions

We analyse particle tracing data from PIC simulations by using neural networks as a tool that can facilitate big data post-processing and analysis in the research of astrophysical shocks. We perform regression and anomaly detection by using a CNN and an auto-encoder. Regression was able to predict extremely well the energies of particles as seen through linear regression, achieving an $R^2 = 0.9892$. On the other hand, anomaly detection can detect energetic particles without the need of a label. Approximately half of the energetic particles that we obtain from the prediction will be true energetic particles.

Acknowledgements: This work has been supported by Narodowe Centrum Nauki through research project 2019/33/B/ST9/02569. This research was supported by the PLGrid infrastructure through grant “plgastrogpu22”.

References

1. A. Bohdan, J. Niemiec, M. Pohl, Y. Matsumoto, T. Amano and M. Hoshino: Astrophysical J., 2019, 878:5.
2 . Y. Yang, K. Zha, Y. Chen, H. Wang and D. Katabi: Delving into Deep Imbalanced Regression. ICML conference, July 18-24, 2021. GitHub: `https://github.com/YyzHarry/imbalanced-regression`

Dog Gait Assessment Using Temporal Graph Neural Networks

Szymon Mazurek[1], Krystian Strzałka[1], Maciej Wielgosz[1,2], Jakub Caputa[1], Rafał Frączek[1,2], Michał Karwatowski[1,2], Jakub Grzeszczyk[1], Jan Krupiński[1], Daria Łukasik[1], Anna Śmiech[3], Paweł Russek[1,2], Agnieszka Dąbrowska-Boruch[1,2], Ernest Jamro[1,2], Marcin Pietroń[1,2], Sebastian Koryciak[1,2], Kazimierz Wiatr[1,2]

[1] ACC Cyfronet AGH, Nawojki 11, 30-950 Kraków, Poland
[2] AGH University of Science and Technology, al. Mickiewicza 30, 30-059 Kraków, Poland
[3] University of Life Sciences, al. Akademicka 13, 20-950 Lublin, Poland

s.mazurek@cyfronet.pl,
anna.smiech@up.lublin.pl,
{rafalfr, mkarwat, wielgosz, russek, adabrow, jamro, pietron, koryciak, wiatr}@agh.edu.pl, {k.strzalka, j.krupinski, d.lukasik, j.grzeszczyk, j.caputa}@cyfronet.pl

Keywords: dog hip dysplasia, deep learning, graph neural network, computational veterinary medicine

1. Introduction

Dog hip dysplasia is a genetic condition where the hip joint does not develop properly, causing instability and degeneration of the joint over time. Diagnosis of hip dysplasia in dogs is typically made through a combination of physical examination and X-rays. Each of these methods requires usage of advanced diagnostic devices or the participation of trained physicians. The purpose of our work is to create a reliable and lightweight model that will be able to classify the gait of a dog based on the video. We are aiming to involve this model as a part of the broader examination pipeline, shown in Fig. 1. below.

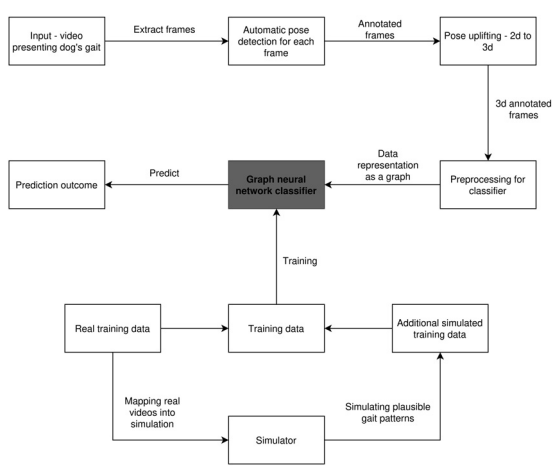

Fig. 1. Overview of the whole diagnostic system that this work is a part of.

2. Description of the problem

The problem is to perform binary classification on a set of frames gathered from the video presenting the dog's gait. Due to the scarcity of data on properly recorded dogs with hip dysplasia walking, the experiments were performed using simulation data. The data contained two

types of videos – healthy and abnormal. The abnormal gait was simulated by manipulating the movement of the back hip and leg movements in the model of normal gait. For every frame, the dog's key joints were annotated automatically by the simulator engine for both 2d and 3d positions. The videos consisted of 150 frames each. 14 and 16 videos were generated for healthy and abnormal gaits, respectively.

3. Solution of the problem

The dog posture in each frame was represented as a graph, with nodes representing the joints and edges created according to the joint connections in real dogs. The frames were then stacked sequentially to include the temporal dimension, allowing the assessment of the movement pattern of a given joint across a set of frames. A temporal graph neural network was chosen to assess the frames and relationships between them.

As a part of preprocessing, the coordinates were z-standardized among temporal dimensions for every joint separately, as this approach was noted to shorten the time necessary for the network to converge and improve the final results [1].

The network consisted of an attention based graph convolution layer [2] as the feature extractor with ReLu activation. The outputs from the feature extractor were then flattened and passed through a dense layer. AdamW optimizer with learning rate of 0.002 and weight decay of 0.001 was used to minimize binary cross entropy loss. Batch size was set to 8. Early stopping mechanism was adapted, stopping the training if no improvement of validation loss was noted for 3 epochs.

The network was created using the Pytorch Geometric Temporal [3] library 2.2.0 for Python 3.10. The inherent benefit of graph neural networks is their small size, therefore the experiments could be run using only 4 CPUs and 20 GB RAM memory on Ares supercomputer.

The performance of the network was assessed for different sample lengths using 10-fold stratified cross validation. For each fold, 70% of the data was used as a training subset, 15% as validation subset and 15% as test subsets. The training, validation and test samples were randomly chosen from the videos. The results have shown that the model performed better on 3d data for every timestep length. The best performance was reached on 5 frame timestep samples, reaching accuracy of 100% and AUROC of 1 for 3d data and 97% and 1 for 2d data for the same metrics respectively. Increasing the length of the samples degraded the performance for both 2d and 3d data, with 3d data providing better results for every timestep chosen.

To further assess the robustness of the model, the creation of the testing and validation subsets was modified to the leave-n-out approach. This time, entire recordings were subtracted from the training set for testing and validation to assess how the model will perform on previously unseen videos. Once again 70/15/15 split ratio was used to create training, testing and validation subsets respectively. Surprisingly, this setting showed better performance in terms of accuracy and AUROC for 2d data, reaching 79% and 0.8 for the metrics respectively, while 3d data reached 63% and 0.61. The best results occurred once again using 5 frames per sample. As previously, increasing the frames per sample led to performance degradation, with 3d data performing better than 2d for longer samples.

4. Conclusions

Obtained results provide a proof of concept that a temporal graph attention network is capable of classifying movement patterns across frames on simulated data presenting a dog's gait. The performance decreases with increasing number of frames per sample, indicating that long term dependencies are harder for a model to capture. This could potentially be relieved by increasing the model's size, although further investigation is necessary. The performance supports the initial hypothesis that providing 3d coordinates of the dog's body key points will carry more information about the gait pattern, therefore increasing the performance.

Acknowledgements. PLGrid grant ID: plglaoisi23.

References

1. Bai, Jiandong, Jiawei Zhu, Yujiao Song, Ling Zhao, Zhixiang Hou, Ronghua Du, and Haifeng Li. 2021. "A3T-GCN: Attention Temporal Graph Convolutional Network for Traffic Forecasting" ISPRS International Journal of Geo-Information 10, no. 7: 485. https://doi.org/10.3390/ijgi10070485
2. Aderinola, Timilehin B. and Connie, Tee and Ong, Thian Song and Teoh, Andrew Beng Jin and Goh, Michael Kah Ong. 2022."Gait-based Age Group Classification with Adaptive Graph Neural Network". https://doi.org/10.48550/arXiv.2210.00294
3. Rozemberczki, Benedek and Scherer, Paul and He, Yixuan and Panagopoulos, George and Riedel, Alexander and Astefanoaei, Maria and Kiss, Oliver and Beres, Ferenc and López, Guzmán and Collignon, Nicolas and Sarkar, Rik. 2021. "PyTorch Geometric Temporal: Spatiotemporal Signal Processing with Neural Machine Learning Models". https://doi.org/10.48550/arXiv.2104.07788

Do Cohort Studies in Diffusion MRI Require a Marriage of Convenience with High-Performance Computing? A Case Study

Dominika Ciupek[1], Julia Machnio[1,2], Maciej Malawski[1,2], Tomasz Pięciak[3]

[1] Sano Centre for Computational Medicine, 30-054 Kraków, Poland
[2] AGH University of Science and Technology, al. Mickiewicza 30, 30-059 Kraków, Poland
[3] Universidad de Valladolid, Valladolid, 47011 Spain

{d.ciupek, m.malawski}@sanoscience.org, julia.machnio@student.agh.edu.pl, tpieciak@tel.uva.es

Keywords: diffusion MRI, tractography, brain ageing, microstructural parameters

1. Introduction

Diffusion Magnetic Resonance Imaging (dMRI) is a non-invasive medical modality that explores fibrous tissue architecture based on measuring molecules' movement [1]. dMRI has already been used to study brain alterations due to pathological changes [2] and natural processes of development and ageing [3] by probing tissue quantitatively using microstructural parameters or qualitatively through the geometrical-based neuroarchitecture. Regular cohort analysis in clinical studies with dMRI involves hundreds of thousands of multidimensional samples (see Fig. 1.) and multivariate model fitting procedures applied on a voxel-by-voxel basis making it infeasible to be handled with a typical workstation [4]. This work explores the acceleration outcomes from translating computationally demanding tasks from dMRI pipeline processing to a high-performance computing centre.

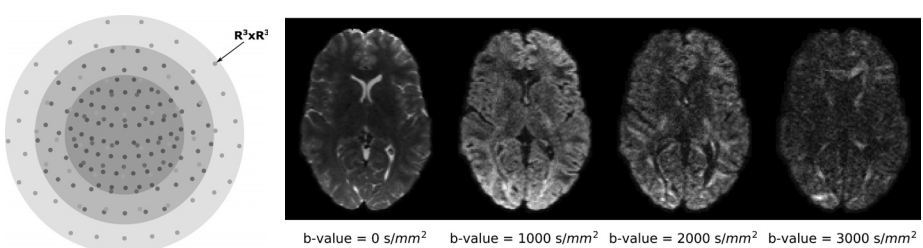

Fig. 1. (a) The acquisition space in dMRI and (b) exemplary images acquired under different b-values.

2. Model optimization on a voxel-by-voxel basis

The microstructure quantities in dMRI can be resolved, for instance, *via* the biophysical models, with the NODDI [5] being an illustrative of multi-compartment tissue structure:

$$f(b, f_{\mathrm{i}}, f_{\mathrm{fw}}, \kappa, \mu) = (1 - f_{\mathrm{fw}})(f_{\mathrm{i}}S_{\mathrm{i}} + (1 - f_{\mathrm{i}})S_{\mathrm{e}}) + f_{\mathrm{fw}}S_{\mathrm{fw}}, \tag{1}$$

where b is the b-value (i.e., acquisition parameter), f_{fw} and f_{i} are isotropic and intra-neurite volume fractions, respectively, S_{fw}, S_{i}, and S_{e} are isotropic, intra-, and extra-neurite signals. The model (1) is solved on a voxel-by-voxel basis *via* the regularized least squares:

$$\mathrm{argmin}_{\mathbf{x}\geq 0}\|\mathbf{\Phi x} - \mathbf{y}\|^2 + \lambda R(\mathbf{x}) \tag{2}$$

with **x** being the vector of the volume fractions, **y** is the vector of dMRI signals, $||.||^2$ is the Euclidean norm in R^n and $R(\mathbf{x})$ is the regularization operator.

3. Results and conclusions

The cohort included a group of 62 healthy subjects aged 8-75y. For each subject, we optimized (1) the NODDI model using high-performance computing, while (2) the tractography and (3) the registration of the geometrical tracts to the Montreal Neurological Institute (MNI) common space was resolved domestically. The computation time for NODDI analysis with a personal computer for a single subject is at ~13.5h, while its computation on the Ares system lasts ~15h. Despite longer computation time on the Ares system, it allows for parallel computing of the NODDI model for the cohort sample at ~15h instead of ~837h intended for linear processing, making it impossible with an in-home condition.

To visualize one of the measures (i.e., f_i), the geometrical-based neuroarchitecture was resolved using an anatomically constrained solution (MRTrix3) combined with SIFT tract filtering technique (MRTrix3). The microstructure measures were combined with geometrical tracts with rigid transformation using 12 degrees of freedom to the MNI space (see Fig. 2.).

Fig. 2. Intra-neurite volume fraction f_i changes along the right arcuate fasciculus across the adult lifespan.

Acknowledgements. The numerical experiment was possible through computing allocation on the Prometheus and Ares system at ACC Cyfronet AGH under the grants PLG/2022/015357 and PLG/2023/016117. Tomasz Pieciak acknowledges the Polish National Agency for Academic Exchange for grant PPN/BEK/2019/1/00421 under the Bekker programme and the Ministry of Science and Higher Education (Poland) under the scholarship for outstanding young scientists (692/STY/13/2018). This work is supported by the European Union's Horizon 2020 research and innovation program under grant agreement Sano No 857533 and the International Research Agendas program of the Foundation for Polish Science.

References

1. P. J. Basser, J. Mattiello, and D. LeBihan: "MR diffusion tensor spectroscopy and imaging". Biophysical journal, 66(1), 1994, pp.259-267.
2. M. Kubicki, R. McCarley, C.-F. Westin, H.-J. Park, S. Maier, R. Kikinis, F. A. Jolesz, and M. E. Shenton: "A review of diffusion tensor imaging studies in schizophrenia". Journal of psychiatric research, 41(1-2), 2007, pp.15-30.
3. D. Beck, A. G. de Lange, I. I. Maximov, G. Richard, O. A. Andreassen, J. E. Nordvik, and L. T. Westlye: "White matter microstructure across the adult lifespan: A mixed longitudinal and cross-sectional study using advanced diffusion models and brain-age prediction". NeuroImage, 224, 2021.
4. M. Hernandez-Fernandez, I. Reguly, S. Jbabdi, M. Giles, S. Smith, S., and S. N. Sotiropoulos: "Using GPUs to accelerate computational diffusion MRI: From microstructure estimation to tractography and connectomes". NeuroImage, 188, 2019, pp.598-615.
5. H. Zhang, T. Schneider, C. A. Wheeler-Kingshott, and D. C. Alexander: "NODDI: practical in vivo neurite orientation dispersion and density imaging of the human brain". NeuroImage, 61(4), 2012, pp.1000-1016.

Classification of Images of Cytological Samples for the Purposes of Initial Analysis

Jan Krupiński[1], Szymon Mazurek[1], Krystian Strzałka[1], Maciej Wielgosz[1,2], Jakub Caputa[1], Rafał Frączek[1,2], Michał Karwatowski[1,2], Jakub Grzeszczyk[1], Daria Łukasik[1], Anna Śmiech[3], Paweł Russek[1,2], Agnieszka Dąbrowska-Boruch[1,2], Ernest Jamro[1,2], Marcin Pietroń[1,2], Sebastian Koryciak[1,2], Kazimierz Wiatr[1,2]

[1] ACC Cyfronet AGH, Nawojki 11, 30-950 Kraków, Poland
[2] AGH University of Science and Technology, al. Mickiewicza 30, 30-059 Kraków, Poland
[3] University of Life Sciences, al. Akademicka 13, 20-950 Lublin, Poland

j.krupinski@cyfronet.pl,
anna.smiech@up.lublin.pl,
{rafalfr, mkarwat, wielgosz, russek, adabrow, jamro, pietron, koryciak, wiatr}@agh.edu.pl, {s.mazurek, k.strzalka, d.lukasik, j.grzeszczyk, j.caputa}@cyfronet.pl

Keywords: cytology, classification, deep learning

1. Introduction

The CyfroVet project [1] aims to develop a system for automatic diagnosis using the images of cytological samples submitted by a veterinarian. Such images could possess many defects which could negatively impact the classification of the cells by a machine learning model. In this research we propose the use of preliminary classification of images to detect the most common issues, so they could potentially be remedied.

2. Description of the problem

The images submitted by the user could possess various defects. The most common issue is that the relevant cells are out of focus. Due to the three-dimensional nature of the cell sample, irrelevant parts of the image could still be in focus, thus, judging the overall sharpness of the image is not enough. Other image defects are less common, or less impactful. Furthermore, the system also needs to be protected from accepting random images, which could produce equally random results.

3. Solution of the problem

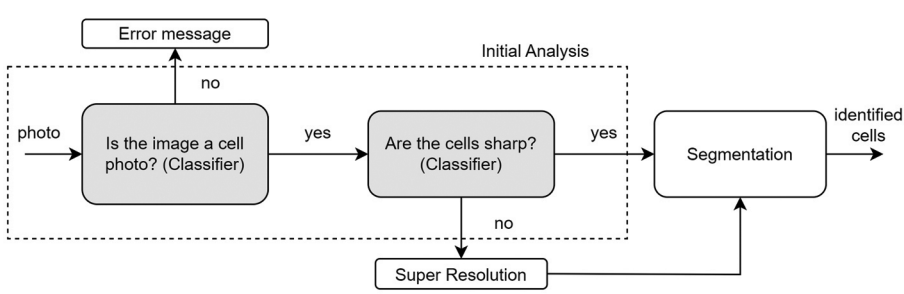

Fig. 1. Proposed pipeline.

The proposed pipeline is presented on Fig. 1. In order to detect non-cytological images, a ResNet [2] model was trained on the collected cytological samples [3] and on the most similar images from the ImageNet [4] dataset.

Another classifier was trained to detect unsharp images using a set of 2600 image pairs of the same sample [3]. The pairs of sharp and unsharp images were crucial in training. The approach producing the best results divided the image into 500x500 segments and summed the outputs of the model using the saturation variance as a weight:

$$\text{prediction} = \text{argmax}(\sum_i \text{var}_i \frac{\text{area}_i}{\text{max .area}} [hr_i \; lr_i])$$

Eq. 1. Ensemble prediction scheme, where *hr* and *lr* are the "*sharp*" and "*unsharp*" outputs.

4. Conclusions

The sharpness classifier reached an accuracy of 97.3%, while the other classifier correctly identified all the cell images from the dataset, as well as 99.25% of 50 000 random images from the ImageNet dataset.

Acknowledgements. The experiment was possible through computing allocation on the Prometheus system at ACC Cyfronet AGH under the grant plglaoisi22.

References

1. J. Caputa, D. Łukasik, M. Wielgosz, M. Karwatowski, R. Frączek, P. Russek, K. Wiatr: "Fast Pre-Diagnosis of Neoplastic Changes in Cytology Images Using Machine Learning", in Applied Sciences, 2021; 11(16):7181. https://doi.org/10.3390/app11167181
2. K. He, X. Zhang, S. Ren, J. Sun: "Deep Residual Learning for Image Recognition", in arXiv:1512.03385
3. Cytology dataset by D. Łukasik: https://git.plgrid.pl/projects/CYFROVET/repos/dataset-superresolution/browse
4. J. Deng, W. Dong, R. Socher, L.-J. Li, K. Li, L. Fei-fei: "Imagenet: A large-scale hierarchical image database.", in 2009 IEEE conference on computer vision and pattern recognition. pp. 248-255.

Leveraging ACC Resources for Medical Research

Piotr Nowakowski[1,2], Marian Bubak[1,2], Krzysztof Gądek[2], Marek Kasztelnik[1], Maciej Malawski[1,2], Jan Meizner[1,2], Adam Nowak[2], Piotr Połeć[1], Karol Zając[2], Taras Zhyulin[2]

[1] IInstitute of Nuclear Physics Polish Academy of Sciences, Radzikowskiego 152, 31-342 Kraków, Poland
[2] Sano Centre for Computational Medicine, Czarnowiejska 36, 30-054 Kraków, Poland

{p.nowakowski, k.gadek, m.malawski, j.meizner, a.nowak, k.zajac, t.zhyulin}@sanoscience.org, {m.kasztelnik, p.polec}@cyfronet.pl

Keywords: high performance computing, medical simulations, digital twins

1. Introduction

Medical simulations are an important area of activity of both ACC Cyfronet AGH and the recently founded Sano Centre for Computational Medicine. In this paper, we present our approach to implementing and deploying advanced features in a computational architecture which is used to enable such simulations.

2. Description of the problem

Recently, in the framework of research projects which focus on the concept of the Human Digital Twin – which is currently gaining popularity [1,2] – researchers face the need to efficiently process large-scale verification and validation studies for computational models which face prospective use in clinical trials. To this end, a suitable computational architecture is required, comprising all layers of the technology stack, from hardware resources to end--user UIs.

3. Solution of the problem

The medical simulations which we're dealing with come from several EU-funded and national research projects centered around the design of Digital Twins and DSS for various specific ailments and treatment procedures, including bone fracture risk prediction, simulation of cerebral aneurisms, digital angiography, and others. The platform which we have built and deployed at ACC Cyfronet AGH is able to efficiently leverage HPC resources to process simulations for patient cohorts, for which a set of simulation campaigns can be carried out [3]. The platform is built on top of the Model Execution Environment solution, previously developed at ACC, which has now been extended with support for creation and management of cohorts and campaigns, as well as integration with new additions to the HPC lineup at ACC.

4. Conclusions

Our success in deploying and executing Digital Twin simulations on ACC infrastructure paves the way to successful verification, validation, and uncertainty quantification of various medical models, which is a necessary step in raising their respective TRL levels and enabling follow-up clinical trials, with a view towards use in the real-life clinical setting [4,5].

Acknowledgements. This work was supported by the EU project ISW under H2020 grant agreement No. 101016503. We gratefully acknowledge Poland's high-performance computing infrastructure PLGrid (HPC Centers: ACC Cyfronet AGH) for providing computer facilities and support within computational grant no. PLG/2022/015279.

References

1. Conference: VIRTUAL PHYSIOLOGICAL HUMAN – Digital twins for personalized treatment development and clinical trials, 6-9 September 2022, https://vph-conference.org/
2. EDITH European Virtual Human Twin, https://www.edith-csa.eu/
3. M. Kasztelnik et al.: Digital Twin Simulation Development and Execution on HPC Infrastructures, submitted to the ICCS 2023 conference (pending).
4. PRIMAGE Project, https://www.primageproject.eu/
5. ISW – In Silico World EU Project, https://insilico.world/

Towards Observability in Scientific Computing

Bartosz Baliś[1,2,3], Albert Kuźma[1], Łukasz Wroński[1]

[1] Sano Centre for Computational Medicine, 30-054 Kraków, Poland
[2] AGH University of Science and Technology, al. Mickiewicza 30, 30-059 Kraków, Poland, Institute of Computer Science
[3] ACC Cyfronet AGH, Nawojki 11, 30-950 Kraków, Poland

{b.balis, a.kuzma, l.wronski}@sanoscience.org

Keywords: observability, scientific computing, HPC, tracing, logging, monitoring

1. Introduction

Large-scale computing systems produce a vast amount of monitoring data whose understanding is vital for detecting performance bottlenecks, identifying root cause of problems, etc. It is argued that traditional monitoring, which focuses on *expected problems*, is no longer sufficient. Consequently, *observability* refers to the techniques and tools that facilitate collecting rich telemetry data and analyzing it in order to discover unexpected problems, or even "unknown unknowns" about the underlying computer systems and applications [1]. Here we demonstrate the application of modern observability principles and tools to scientific computing in a HPC system. This research is done in the context of the InSilicoWorld project[1] and the computing infrastructure of the ACC Cyfronet AGH.

2. Observability framework for scientific computing

The InSilicoWorld project leverages HPC systems to run various applications related to computational medicine. One of the challenges is the diversity of these applications in terms of their execution environments, used software packages, and complexity (workflows, multi-job workloads, etc.). Fig. 1. shows the proposed framework for the observability of such applications. The framework enables three pillars of observability: monitoring (metrics), tracing (end-to-end tracking of distributed requests), and logging (logs generated by individual components). Collecting, processing, and correlating diverse data coming from these three sources is crucial for observability. In our system, jobs are submitted using the *Model Execution Environment* (MEE) tool [2]. Job requests are then forwarded to the *Rimrock* service, the *SLURM workload manager*, and finally to the nodes of the Ares supercomputer in Cyfronet. We instrument all these components, including the SLURM job scripts, using OpenTelemetry tools, to enable end-to-end tracing. Metrics, logs, and trace data are collected by the *Open Telemetry Collector*, processed by *Data Prepper*, and passed to the central *OpenSearch data backend,* which provides long-term storage, querying capabilities, and customizable dashboards. We also use dedicated tools for visualizing metrics (*Prometheus*) and traces (*Jaeger*).

[1] InSilicoWorld: https://insilico.world

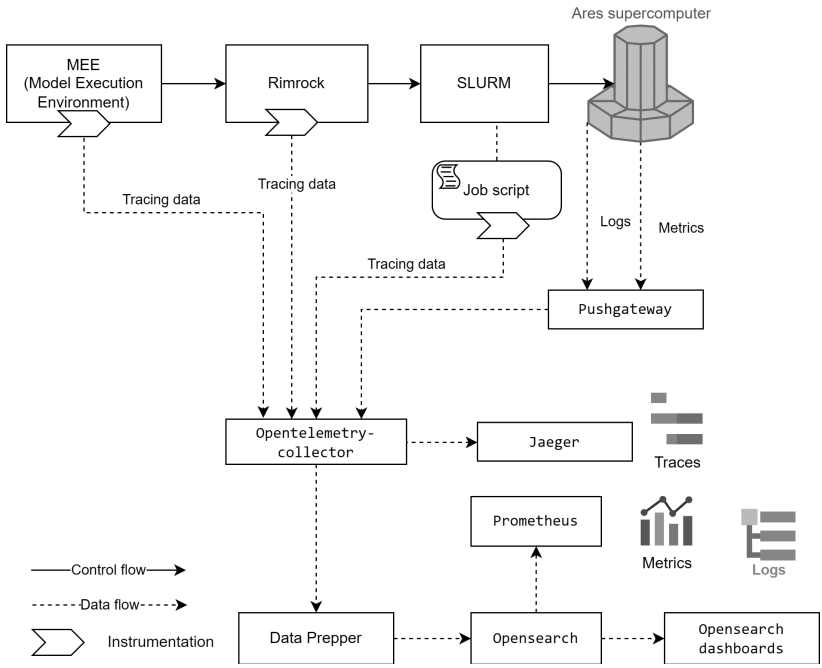

Fig. 1. Observability framework for scientific computing.

3. Conclusions

Observability is widely used in cloud computing, but it is still not widely adopted in the context of scientific computing on HPC systems. Our framework aims to fill this gap. The next step of our research is to use the proposed framework for application performance monitoring using advanced data analytics enabled by the observability system.

Acknowledgements. The work is partly supported by the EU H2020 grant Sano (No. 857533), the IRAP Plus programme of the Foundation for Polish Science; and by the EU project ISW under H2020 grant agreement No. 101016503. We gratefully acknowledge Poland's high-performance computing infrastructure PLGrid (HPC Centers: ACC Cyfronet AGH) for providing computer facilities and support within computational grant no. PLG/2022/015396.

References

1. Niedermaier, S., Koetter, F., Freymann, A., & Wagner, S. (2019). On observability and monitoring of distributed systems–an industry interview study. In Service-Oriented Computing: 17th International Conference, ICSOC 2019, Toulouse, France, October 28–31, 2019, Proceedings 17 (pp. 36-52). Springer International Publishing.
2. Bubak, M., Czechowicz, K., Gubała, T., Hose, D. R., Kasztelnik, M., Malawski, M., ... & Wood, S. (2021). The EurValve model execution environment. Interface Focus, 11(1), 20200006.

UWLCM – Eulerian-Lagrangian Cloud Model for Heterogeneous Computing Clusters

Piotr Dziekan, Piotr Żmijewski

University of Warsaw, Faculty of Physics, Warsaw, Poland

{pdziekan, p.zmijewski2}@fuw.edu.pl

Keywords: cloud modeling, large-eddy simulations, GPU, scalability

1. Introduction

Understanding atmospheric clouds is important for weather and climate predictions. Numerical modeling is one of the methods for studying clouds. University of Warsaw Lagrangian Cloud Model (UWLCM) is a tool for modeling individual clouds and cloud fields. Highlights of UWLCM are: detailed modeling of cloud droplets and simultaneous use of CPUs and GPUs. We present how UWLCM was adapted for distributed memory systems and how it scales to multiple nodes.

2. Description of the problem

To model clouds, it is necessary to model air flow and droplets. In the University of Warsaw, Lagrangian Cloud Model (UWLCM) droplets are modeled using a novel Lagrangian method, and dynamics are modeled in an Eulerian manner. Lagrangian calculations can be done either by CPUs or GPUs, while Eulerian calculations are done by CPUs. Differences in the number, computing power and memory size between CPUs and GPUs make it challenging to efficiently run the model on multiple nodes.

3. Solution of the problem

The modeled domain is divided between MPI processes along one dimension, which was found to give the best performance of GPU-to-GPU communications. Each MPI process can control multiple CPUs and GPUs, using further decomposition between these processing units, but along the other dimension than decomposition between MPI processes.

Lagrangian computations scale better than Eulerian computations. For this reason, the time CPUs and GPUs are simultaneously used depends not only on simulation parameters, but also on the number of processes.

4. Conclusions

Meaningful scientific simulations on multiple nodes can use CPUs and GPUs simultaneously for up to 80% of the simulation time.

Acknowledgements. Work was supported by the Polish National Science Center (grant no. 2018/31/D/ST10/01577). The numerical experiment was possible through computing allocations at ACC Cyfronet AGH (grants plguwlcmscale and uwlcmmpire) and at ICM UW.

References

1. P. Dziekan and P. Zmijewski, *Geosci. Model Dev.*, 15, 4489–4501, 2022.

Unsupervised Detection of Decoupled Subspaces in the Quantum Hilbert Space

Tomasz Szołdra[1,2], Piotr Sierant[3], Maciej Lewenstein[3,4], Jakub Zakrzewski[2,5]

[1] Szkoła Doktorska Nauk Ścisłych i Przyrodniczych, Uniwersytet Jagielloński, Łojasiewicza 11, PL-30-348 Kraków, Poland
[2] Instytut Fizyki Teoretycznej, Uniwersytet Jagielloński, Łojasiewicza 11, 30-348 Kraków, Poland
[3] ICFO-Institut de Ciencies Fotòniques, The Barcelona Institute of Science and Technology, Av. Carl Friedrich Gauss 3, 08860 Castelldefels (Barcelona), Spain
[4] ICREA, Passeig Lluis Companys 23, 08010 Barcelona, Spain
[5] Mark Kac Complex Systems Research Center, Uniwersytet Jagielloński, PL-30-348 Kraków, Poland

tomasz.szoldra@doctoral.uj.edu.pl, {psierant, maciej.lewenstein}@icfo.net, jakub.zakrzewski@uj.edu.pl

Keywords: quantum machine learning, autoencoder, many-body, scars, clusterization

1. Introduction

Recent progress in noisy, intermediate scale quantum (NISQ) computers [1] lead to fast development of algorithms suited for use on them [2] in various areas: physics, machine learning, quantum chemistry, and combinatorial optimization. In this work, we demonstrate the applicability of quantum variational autoencoders (QVAE) in an analysis of properties of highly excited eigenstates in quantum many-body systems.

2. Description of the problem

Highly excited eigenstates of a generic quantum many-body Hamiltonian are usually those of a random ensemble, but some systems possess a small number of special eigenstates, called "scars", that live in a decoupled region of the Hilbert space. Scars are hosted, e.g., by a chain of Rydberg atoms, described by the spin-1/2 Hamiltonian**,**

$$H = \sum_i P_{i-1}\sigma_i^x P_{i+1}, \qquad (1)$$

where $P_i = (1-\sigma_i^z)/2$ and $\sigma_i^{x,y,z}$ are Pauli matrices for the -th spin. Our task is to find scars that belong to the same decoupled subspace.

3. Solution of the problem

We train a QVAE, presented in Fig. 1a), to compress each eigenstate of into a smaller number of qubits than we start with. Then, we expect that eigenstates "similar" to the one we trained on will be compressible in a similar way. Looking at compression losses, we can discover clusters of related eigenstates, see Fig. 1b) and c), some of which were not described in the literature.

We use the IBM Qiskit framework [4] to optimize the parameters of quantum circuits. Our custom implementation of constrained Hilbert space allows us to reach system sizes of 24 qubits, with a total consumed time of ~50k CPU hours in the *plgauge2* grant. For ease of deployment, we use Singularity containers [5], now available in our repository [6].

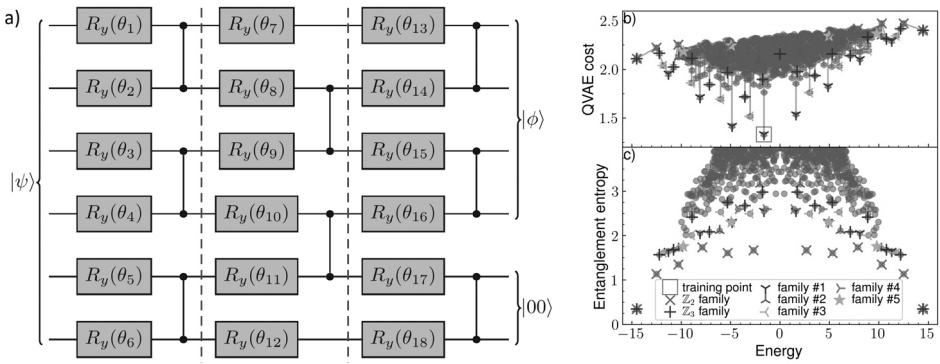

Fig. 1. a) Architecture of the QVAE circuit composed of single-qubit rotations and controlled-Z gates. b) Compression of a special eigenstate of the Rydberg atom chain of size 24 reveals other eigenstates from the same subspace. c) Families of special "scar" eigenstates are identified. Most of them are characterized by a low von Neuman entanglement entropy.

4. Conclusions

We proposed and validated a quantum machine learning algorithm that allowed us to clusterize untypical eigenstates in quantum many-body systems. Our method can be applied to any model hosting decoupled subspaces.

Acknowledgements. This research was partially funded by the Digiworld under the program Excellence Initiative – Research University at the Jagiellonian University in Krakow. The works of T. S. and J. Z. have been realized within the grant 2019/35/B/ST2/00034 of NCN (Poland). P. S. and M. L. acknowledge support from: ERC AdG NOQIA; Agencia Estatal de Investigación; Fundació Cellex; Fundació Mir-Puig; Generalitat de Catalunya through the European Social Fund FEDER and CERCA; European Union's Horizon 2020. The numerical experiment was possible through computing allocation on the Prometheus system at ACC Cyfronet AGH under the grant *plgauge2*.

References

1. J. Preskill: Quantum computing in the NISQ era and beyond. in Quantum 2, 79, 2003.
2. K. Bharti et al.: Noisy intermediate-scale quantum algorithms. in Rev. Mod. Phys. 94, 015004, 2022.
3. T. Szołdra, P. Sierant, M. Lewenstein, and J. Zakrzewski: Unsupervised detection of decoupled subspaces: Many-body scars and beyond. in Phys. Rev. B 105, 224205, 2022.
4. Qiskit, `https://qiskit.org`
5. Singularity, `https://sylabs.io`
6. OpenData catalog, `https://chaos.if.uj.edu.pl`

Scalability of a Neuroevolutionary Based Framework for Anomaly Detection

Marcin Pietroń[1,2], Dominik Żurek[3], Kamil Faber[3]

[1] AGH University of Science and Technology, al. Mickiewicza 30, 30-059 Kraków, Poland, Institute of Electronics
[2] ACC Cyfronet AGH, Nawojki 11, 30-950 Kraków, Poland
[3] AGH University of Science and Technology, al. Mickiewicza 30, 30-059 Kraków, Poland, Institute of Computer Science

{pietron, dzurek, kfaber}@agh.edu.pl

Keywords: deep learning, neuroevolution, anomaly detection, autoencoders

1. Introduction

Anomaly detection tools and methods present a key capability in modern failure prediction systems. The deep learning architectures outperform other machine learning models in this field on complex datasets. However, existing deep learning approaches mostly focus on optimizing model architectures without taking into account feature subspaces. We describe a scalable multi-level optimized neuroevolution framework for time series anomaly detection. The method optimizes feature subspaces for an ensemble model, optimizes the model architecture, and performs non-gradient fine-tuning of network weights.

2. Description of the problem

The anomaly detection model optimization for a given dataset is a cumbersome and time consuming process. Neuroevolution could be an effective and efficient solution to this problem, as a fully automated search method for learning optimal neural autoencoders. The next advantage is its high scalability.

3. Solution of the problem

The starting point of the framework is data preparation – which consists of downsampling training data used in the following evolution levels, and splitting it into overlapping windows, which reduces the computational cost of the following steps. The next step is finding the optimal partition of input features into subspaces, leading to an effective matching between features and models. After that, model evolution is performed. As the next level, the best model for each subspace extracted from the previous level is fine-tuned using the non-gradient genetic optimization method. Subsequently, the ensemble model combines all fine-tuned models evaluating them using a voting mechanism. Experiments on widely adopted multivariate anomaly detection benchmark datasets show that the models extracted by the framework outperform the best deep learning architectures (GNN [1], UAE [3] and USAD [4], Table 1). The experiments were run in ten trials and mean value is presented in Table 1 (the variance is 0.005). Moreover, results show that the proposed method can perform the whole process efficiently, presenting high scalability when multiple GPUs are available.

Tab. 1. Comparison of *F1* score on WADI and SWAT benchmarks.

Method	WADI	SWAT
GNN[1]	0.57	0.81
UAE[3]	0.47	0.58
USAD[4]	0.43	0.79
Ours	**0.59**	**0.82**

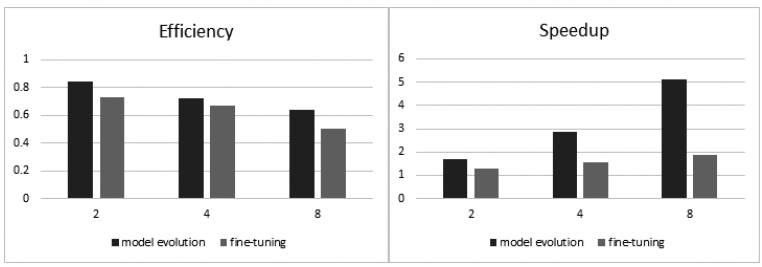

Fig. 1. Framework scalability (on x-axis number of GPUs), experiments run in isolated mode.

4. Conclusions

An extensive experimental evaluation results show that the final ensemble model generated by the neuroevolution framework outperforms state-of-the-art anomaly detection models for time series anomaly detection. The framework execution can be seamlessly scaled up by adding computational resources.

Acknowledgements. This research was partially supported by the PLGrid infrastructure (plglaoisi23).

References

1. A. Deng and B. Hooi: „Graph Neural Network-Based Anomaly Detection in Multivariate Time Series". in Proc. AAAI International Conference on Artificial Intelligence, 2021.
2. K. Faber, M. Pietron and D. Zurek: „Ensemble Neuroevolution-Based Approach for Multivariate Time Series Anomaly Detection", Entropy, 2021, November, vol. 23 (11).
3. A. Garg, W. Zhang, J. Samaran, R. Savitha, and C-S. Foo: „Graph Neural Network-Based Anomaly Detection in Multivariate Time Series", An Evaluation of Anomaly Detection and Diagnosis in Multivariate Time Series, IEEE Transactions on Neural Networks and Learning Systems, 2022.
4. J. Audibert, P. Michiardi, F. Guyard, S. Marti and M. A. Zuluaga: „USAD: UnSupervised Anomaly Detection on Multivariate Time Series", Proceedings of the ACM SIGKDD 2020, p. 3395–3404.

Author Index

Notes

Published by

ACC Cyfronet AGH
ul. Nawojki 11
30-950 Kraków
www.cyfronet.pl

Sponsors

ISBN 978-83-61433-37-8